



Université de Lomé



West Africa Science Service Centre on
Climate Change and Adapted Land Use

FACULTY OF ART AND HUMANITIES DEPARTMENT OF GEOGRAPHY

MASTER RESEARCH PROGRAM CLIMATE CHANGE AND HUMAN SECURITY

ASSESSMENT OF MID-CENTURY CLIMATE CHANGE IMPACTS ON MONO RIVER'S DOWNSTREAM INFLOWS.

Thesis N°.....

Thesis submitted in partial fulfilment of the requirements for the award of Masters Research Degree

DOMAIN:	HUMANITY AND SOCIAL SCIENCES
MENTION:	GEOGRAPHY
SPECIALTY:	CLIMATE CHANGE AND HUMAN SECURITY

Presented by: **Nina Rholan HOUNGUE**

Supervisor: Prof Agnidé Emmanuel LAWIN

(Institut National de l'Eau, Université d'Abomey-Calavi)

Approved on January, 30th 2018 by:

Chair of the Committee:	Prof Sidat YAFFA	(University of The Gambia, The Gambia)
Committee Members:	Dr. Edjamé KODJOVI	(Université de Lomé, Togo)
	Dr. Georges ABBEY	(Université de Lomé, Togo)
	Dr. Felix OLORUNFEMI	(Nigerian Institute of Social and Economic Research (NISER), Ibadan, Nigeria)

Director of the Program: Prof. Kouami KOKOU

January, 2018

Dedication

To

The light giver,

I'm like a stranger by a river

You tell me "I am always with you"

And I believe, you help me see through.

Acknowledgement

My sincere appreciation goes to the Federal Ministry of Education and Research (BMBF) and West African Science Centre on Climate Change and Adapted Land Use (WASCAL) for providing the scholarship and financial support for this programme.

I am grateful to the team of WASCAL Togo, the Director Prof Kouami Kokou, the Deputy director Prof Ruben Afagla, Mrs Séfako Ségbé, Mr Folly Kuevi, Mr Codjo and Mr Zarifou. To all the lecturers, thank you for inspiring me. I also express my gratitude to the members of the scientific panel who spared no effort to support the accomplishment of this thesis. I render special thanks to Mrs Fafavi d'Almeida for encouraging and being a model for me; sometimes a gaze or a smile is worthiest than words are.

I owe more than gratitude to my supervisor Prof. Agnidé Emmanuel Lawin who helped me make my first steps in the scientific world, held my hand and taught me to aim high. I am deeply grateful to you. During my stay in Benin I got support from WASCAL graduate research program on Climate Change and Water Resources namely, Prof Jean Adoukpè, Dr Jean Hounkpè, Mrs Imelda Djagoun, Mr. Salem Elégbédé, Dr Komi Kossi, and Mr Yekanbessoun M'Po N'Tcha. My sincere and special acknowledgement to Dr Djigbo Félicien Badou who often enlightens the way for me.

During data collection, I benefited from the help of Mr Félix M'Poh, Mr Eugène Nawanti, Mr Flavien Lanhoussi and Dr Félix Azonsi. Also, have I been supported by the staff of Athiémé's town hall especially the department of general affairs during my field work.

My heartiest thanks to my family. I may ever not reward you as you deserve but I hope you feel honoured and proud through this thesis. My father Raymond Houngue, my mother Lucie Anago-Kpogla, my sisters and brothers Rita, Rhoyale, Mendel, Cessac, Jules, thank you all. I made it with your multiple support.

My fellows offered me a second family during my stay in Togo. Richard Asante, Momodou Badjie, Michel Diop, Namo Lawson Zankli, Grace Lucien Kokoye, Boris Ouattara, Peter Oyedele, Nagalé Sanogo and Jean-Baptiste Sawadogo, thank you all.

I do not forget support from friends: Harold, Brigitte, Jean-Baptiste, Ronald, Judith, Thierry, and Arthur.

Table of Contents

Dedication	ii
Acknowledgement	iii
Abstract.....	x
Résumé.....	xi
CHAPTER I: INTRODUCTION	1
<i>Problem Statement</i>	<i>1</i>
<i>Objectives.....</i>	<i>2</i>
<i>Research Questions.....</i>	<i>3</i>
<i>Hypotheses</i>	<i>3</i>
<i>Thesis Structure.....</i>	<i>3</i>
CHAPTER II: LITERATURE REVIEW	4
<i>2.1. Concepts Clarification</i>	<i>4</i>
<i>2.2. Flood Characteristics, and Climate Trend Analysis in Mono River Watershed ...</i>	<i>4</i>
<i>2.3. Future Climate Data and Bias Correction</i>	<i>5</i>
<i>2.4. Assessment of Climate Change Impact on River’s Discharge.....</i>	<i>7</i>
<i>2.5. Discharge Modelling and Assessment of Climate Change Impact in Mono River watershed</i>	<i>8</i>
CHAPTER III: MATERIAL AND METHODS.....	10
<i>3.1. The Study Area.....</i>	<i>10</i>
<i>3.2. Methods.....</i>	<i>12</i>
3.2.1. Analysis of Past and Future Climate Trend.....	12
3.2.2. Projected Climate Data and Bias Correction.....	15
3.2.3. Discharge Modelling and Projection	16
3.2.4. Assessment of the Impacts of Projected Discharges on Human Security	19
<i>3.3. Data Collection and Analysis</i>	<i>20</i>

3.3.1. Data Collection.....	20
3.3.2. Data Analysis	23
CHAPTER IV: RESULTS AND DISCUSSION.....	26
4.1. <i>Climate in the Mono Watershed.....</i>	26
4.1.1. Observed Climate	26
4.1.2. Projected Climate	31
4.2. <i>Discharge modelling</i>	39
4.2.1. Sensitivity analysis	39
4.2.2. Calibration and validation	40
4.2.4. Expected discharges under RCP 4.5 and RCP 8.5	41
4.3. <i>Implication of Projected Discharges for Infrastructures and Human Security... 43</i>	43
4.3.1. Existing Threats/Background	43
4.3.2. Projected Impacts	46
CHAPTER V: CONCLUSION AND POLICY RECOMMENDATIONS	51
References.....	53
Annexes	59

LIST OF FIGURES

Figure 1. Location of Mono watershed.....	11
Figure 2: Location of Athiémé.....	11
Figure 3: Components of a variogram	13
Figure 4: Variogram models	13
Figure 5: General structure of HBV-light model	17
Figure 6: Rainfall seasonal cycles in Mono watershed.....	26
Figure 7: SNH test performed on observed annual rainfall time series	27
Figure 8: Standardized Precipitation Index (SPI) of observed annual rainfall	28
Figure 9: Pettit’s test and Standardized Normal Homogeneity (SNH) test for temperature	29
Figure 10: Anomaly of mean annual temperature over Mono watershed	29
Figure 11: Trend of maximum discharge at Athiémé and annual rainfall in Mono watershed ...	30
Figure 12: Mean hydrograph of Mono river during 1981-2010	30
Figure 13: Comparison of observed and simulated rainfall.....	32
Figure 14: Comparison of observed and simulated temperature	33
Figure 15: Rainfall seasonal cycles under RCP 4.5 and RCP 8.5	33
Figure 16: Expected change in seasonal cycles under RCP 4.5 and RCP 8.5	34
Figure 17: Pattern of annual rainfall in the southern part under RCP 4.5 and RCP 8.5	35
Figure 18: Pattern of annual rainfall in the central and northern part under RCP 4.5 and RCP 8.5	36
Figure 19: Standardized Precipitation Index of annual rainfall under RCP 4.5 and RCP 8.5	37
Figure 20: Homogeneity tests performed on temperature under RCP 4.5 and RCP 8.5	38

Figure 21: Temperature anomaly under RCP 4.5 and RCP 8.5	39
Figure 22: Sensitivity analysis of the parameters of HBV-light	40
Figure 23: Calibration and validation of HBV-light	40
Figure 24: Projected discharge under RCP 4.5	42
Figure 25: Projected discharge under RCP 8.5	42
Figure 26: Mean hygrograph at Athiémé for the normal period and the period 2018-2050 under RCP 4.5 and RCP 8.5	43
Figure 27: Land use and land cover map	45
Figure 28: Projected maximum discharge under RCP 4.5 and RCP 8.5	46
Figure 29: Flood prone areas in Athiémé from 2020 to 2050	47
Figure 30: Flood prone areas in Athiémé from 2020 to 2050	49

LIST OF TABLES

Table 1: Instances of studies related to climate change impact on river's runoff.....	8
Table 2: Sub-models of HBV-light.....	17
Table 3: Characteristics of REMO2009.....	21
Table 4: Summary of data collected and used in this study.....	22
Table 5: SPI value range and corresponding interpretation.....	24
Table 6: Result of Pettit's and SNH test on observed rainfall.....	27
Table 7: Results of Mann-Kendall test performed on observed annual rainfall.....	27
Table 8: Results of Man-Kendall test on annual rainfall under RCP 4.5 and RCP 8.5.....	34
Table 9: Results of homogeneity tests on annual rainfall under RCP 4.5 and RCP 8.5.....	35
Table 10: Results of Man-Kendall test on annual temperature under RCP 4.5 and RCP 8.5.....	39
Table 11: Evolution of land use/land cover in Mono watershed.....	44
Table 12: Proportion of flood prone areas under RCP 4.5.....	48
Table 13: Proportion of flood prone areas under RCP 8.5.....	50

Acronyms

CENATEL :	Centre National de Télédétection et de Suivi Ecologique du Bénin
CMIP5:	Coupled Model Inter-comparison Project Phase 5
CORDEX:	Coordinated Regional Climate Downscaling Experiment
DEM:	Digital Elevation Model
DGEau :	Direction Générale de l'Eau (Benin)
DMN :	Direction de la Météorologie Nationale
EM-DAT :	Emergency Events Data Base
EQM :	Empirical Quantile Mapping
ETP:	Evapotranspiration
GCM:	Global Climate Model
GDP:	Gross Domestic Product
GPS:	Geographical Positioning System
HBV-light:	Hydrologiska Byråns Vattenbalansavdelning-light
IHMS:	Integrated Hydrological Modelling System
IPCC:	Intergovernmental Panel on Climate Change
NSE:	Nash Sutcliff Efficiency
OK:	Ordinary Kriging
RCM:	Regional Climate Model
RCP:	Representative Concentration Pathway
REMO:	Regional Model
SDG:	Sustainable Development Goal
SNH:	Standard Normal Homogeneity test
SPI:	Standardized Precipitation Index
SRES:	Special Report on Emission Scenarios
SRTM:	Shuttle Radar Topography Mission
UNDP:	United Nations Development Program
UNFCCC:	United Nations Framework Convention on Climate Change
USGS:	United States Geological Survey
WMO:	World Meteorological Organisation

Abstract

In the current context of global climate change and variability, it is important to undertake river flow projection in order to improve watershed management. This is needed to put in place relevant actions in order to improve communities' security. Hence, this study aims at assessing the impact of the mid-century climate change on Mono River downstream inflows at Athiémé (Benin). The projections from the regional climate model REMO, under the scenarios RCP 4.5 and RCP 8.5 were used to force the hydrological model HBV-light. Within the period 2018-2050, temperature will increase and seasonal cycle of rainfall will change throughout the watershed: in the south, the second rainfall peak which normally occurs in September will be extended to October with a higher value; in central and northern parts, there will be late onset of rainfall, shorter rainy season and higher peaks. Consequently, the mean hydrograph will shift rightward, increase in amplitude and the period of high flow will be shortened. Under RCP 4.5, the lowest maximum flow will be recorded in 2031 ($116 \text{ m}^3/\text{s}$) whereas the highest is expected in 2024 ($1236 \text{ m}^3/\text{s}$). Flood prone areas vary between 6.2% to 20.1% of Athiémé's land surface. For RCP 8.5 the lowest maximum flow is projected for 2033 ($123 \text{ m}^3/\text{s}$) and the highest for 2034 ($1150 \text{ m}^3/\text{s}$), with flood prone areas ranging from 6.4% to 19.2%. Thus, it is recommended to undertake thorough risk assessment on one hand, and to account for both high and low flow situations in Mono watershed management strategies.

Key words: Climate projection, Discharge projection, Mono watershed, Athiémé.

Résumé

Compte tenu de l'importance du débit fluvial dans la gestion des bassins versants, et dans le contexte actuel de changement / variabilité climatique, il s'avère important d'entreprendre des projections de débit pour les périodes futures. Ainsi, des mesures appropriées pourraient être mises en place afin d'améliorer la sécurité des communautés. Cette étude vise donc à évaluer l'impact du changement climatique à l'horizon 2050 sur les débits en aval du fleuve Mono à Athiémé (Bénin). Les scénarios RCP 4.5 et RCP 8.5, issus des projections du modèle climatique régional REMO, ont été utilisées pour forcer le modèle hydrologique HBV-light. Les résultats montrent qu'au cours de la période 2018-2050, la température aura une tendance croissante et le cycle saisonnier des pluies connaîtra des modifications dans tout le bassin : au sud, la deuxième saison de pluie s'étendra jusqu'au mois d'Octobre avec un accroissement de pic ; au centre et au nord, il y aura un démarrage tardif des pluies, raccourcissement de la saison de pluie et des pics plus élevés. Par conséquent, l'hydrogramme moyen sera un peu plus décalé vers la droite, avec une augmentation d'amplitude et un raccourcissement de la période des hautes eaux. Avec le scénario RCP 4.5, le plus petit débit de pic surviendra en 2031 ($116 \text{ m}^3/\text{s}$) tandis que la plus forte valeur est attendue pour 2024 ($1236 \text{ m}^3/\text{s}$). Ainsi la superficie des zones susceptibles d'être inondées varie entre 6,2% et 20,1% de la commune d'Athiémé. Par ailleurs, selon le scénario RCP 8.5, le plus petit débit maximal surviendra en 2033 ($123 \text{ m}^3/\text{s}$) et le plus élevé en 2034 ($1150 \text{ m}^3/\text{s}$). La proportion des zones inondables varie de 6,4% à 19,2% de la superficie de la commune. A l'issue de ce travail, il est recommandé d'entreprendre une étude de risque approfondie d'une part, et d'autre part, de tenir compte tant des situations de hautes que de basses eaux dans les stratégies de gestion du bassin du fleuve Mono.

Mots clés : Projections climatiques, Projection de débits, Bassin du Mono, Athiémé.

CHAPTER I: INTRODUCTION

Problem Statement

The importance of water to human livelihood and other living organisms is undeniable. Water bodies such as lakes, rivers, marshes, and oceans provide numerous ecosystem services which are prominent for any life. But only 2.8% of earth's water surface is freshwater, and more worrying, it may be threatened by changes in climate (MEA, 2005).

Exacerbation of climate variability as well as increase of extreme events such as drought, flood, and storms is expected in several regions of the world. The threatened features include environment, health and food security, and generally, human security. In fact, modifications in the climate resulting from both natural and anthropogenic processes have raised considerable concerns (such as more frequent and intense rainfall), as they induce adverse impacts on human and on the whole climate system (IPCC, 2007).

Furthermore, changes in the pattern of climate variables such as precipitation, temperature and evaporation (as a result of climate change) drive modifications in the global water cycle and affect water resources (Bates et al., 2008). It is clear that, the impact of climate change on these climate variables will be both time and region specific (Stocker et al., 2013). Moreover, under the Representative Concentration Pathways (RCP) 4.5, 6.0 and 8.5, the state of climate in various regions may pose a high risk of abrupt and irreversible change in the composition, structure, and function of water resources (IPCC, 2014). This situation will more affect low income countries like those in West Africa, inducing higher fatality rates and economic losses (IPCC, 2012). Climate change has already had substantial impacts on rivers, lakes, flood and/ or drought in West Africa. But the low consensus (from models) on how climate change affects rivers' flow in the region triggers uncertainty and concerns (IPCC, 2007). Therefore, more scientific researches need to be carried out at regional and local levels in West Africa in order to improve preparedness and adaptation strategies.

Indeed, since 1950, flood events in West Africa are recognized to be the most recurrent natural disasters, causing almost 2,384,437 deaths and about 720 billion of dollars (\$) of damages. In Benin, 3,189,547 people have been affected by flood between 1900 and 2016, and almost 40% of them experienced riverine flood (EM-DAT, visited on 17/04/2017). Within the last decade, the

2010 flood event has been recorded as the most disastrous in the country. Total damage and loss are about USD 262 million, representing 2.8% of 2010's annual Gross Domestic Product (GDP) (UNDP, 2011). The impacts hit various sectors such as agriculture, livestock, fisheries, fish farming, health, education and transport. Specifically, 680,000 people were affected, 46 died, 680 tons of agriculture products were lost, as well as 201.600 hectares of crop and 81,000 herds.

These disastrous events stroke many communities, but Athiémé — a town in southern Benin — was heavily impacted. About 75% of the town's population was affected, along with 5024 habitats destroyed, 1300 displaced households and 5,472 ha of agricultural product lost. The case of Athiémé was mainly attributed to the overflow of Mono River. More recently in 2016, 30 villages over 61 faced flood in this town, causing losses of agricultural products, degradation of socio-community infrastructures and outbreak of water-related diseases. Therefore, forecasting Mono River's discharge is required in order to take relevant response and preventive actions with respect to both low and high runoff situations. Hence, people's livelihood may be improved and major challenges could be overcome. More specifically, it will contribute to the achievement of Sustainable Development Goals — SDG2 zero hunger, SDG3 good health and well-being, SDG6 clean water and Sanitation, SDG11 Sustainable cities and communities— and ultimately to human security. Moreover, not only will human being will benefit, but also the surrounding ecosystems and the services they provide –SDG15 life on land, SDG14 life below water.

Objectives

The aim of this study is to explore the impact of climate change on Mono River discharge by 2050.

More specifically, the focus is to:

- analyse the current and future trends of the Mono River watershed climate,
- analyse the impact of the projected climate by 2050 on the Mono River's inflow at its downstream, and
- assess the implications of the projected changes on human security and infrastructures.

Research Questions

Based on the general context of predicted exacerbation of climate variability as well as increase in hydrological disasters at global and regional level, this study addresses the following scientific research questions:

- a) What is the trend of the climate in the Mono River basin and how will it change by 2050?
- b) What will be the potential impacts of climate on the discharge of Mono River by 2050?
- c) What could be the possible implications of the projected discharges on human security and infrastructures?

Hypotheses

This study is based on three hypotheses set as follows:

H1: Climate in the mono river watershed is becoming warmer and dryer;

H2: future climate leads to an increase in the peak flows of the Mono River; and

H3: the increase in peak discharge will negatively affect human security as well as socioeconomic infrastructures.

Thesis Structure

This thesis encompasses five chapters. Chapter one is the introduction which presents the problematic of this research work, the objectives, hypotheses and the core questions tackled. The second chapter explores some concepts and highlights the state of art with respect to three major points: flood characteristics in Mono watershed, analysis of future climate data and climate change impact assessment on river discharge. Chapter three introduces the study area and details the data and methods used to achieve the assigned objectives. The fourth chapter deals with results and discussion while chapter five is devoted to recommendations and conclusion.

CHAPTER II: LITERATURE REVIEW

2.1. Concepts Clarification

Climate Change: UNFCCC defines climate change as “a change of climate which is attributed directly or indirectly to human activity that alters the composition of the global atmosphere and which is in addition to natural climate variability observed over comparable time periods”. This definition differentiates between changes attributable to human activities and those that attributable to natural variability.

The World Meteorological Organization (WMO) also refers to climate change as “a statistically significant variation in either the mean state of the climate or in its variability, persisting for an extended period (typically decades or longer)”.

River Discharge: In the water science glossary of the USGS, discharge is defined as the volume of water that passes a given location within a given period of time. It is usually expressed in cubic feet per second (ft³/s) or cubic meter per second (m³/s).

Model: A model is a simplified representation of a complex system which always describes the basic and most important components of the targeted system (Xu, 2002; Lundin et al., 2000).

2.2. Flood Characteristics, and Climate Trend Analysis in Mono River Watershed

A number of studies have already been conducted on the watershed with respect to flood characteristics and vulnerability assessment. Amoussou (2010) analysed the hydrodynamic of the Mono basin within the period 1961-2000, and noted some key facts. The correlation between rainfall and water discharge in most part of the basin is high. Moreover, inter-annual variability of inflow at Athiémé (with respect to the normal 1961-2000) within a given decade depends on whether that decade counts wet or dry years in terms of rainfall. This finding confirms the conclusion of Sutcliffe and Piper (1986) who reported that runoff in Benin and Togo may be related to seasonal rainfall. However, the amount of water released from the Nangbeto dam has an influence on discharge at the downstream (Rossi et Blivi 1995; Rossi, 1989). Besides, the

geological characteristics of the basin (soil characteristics) and anthropogenic actions –such as deforestation, anarchic settlements— should also be taken into account (Amoussou, 2010; Kissi, 2014). Even if disaster events related to flood depend on anthropogenic actions (Duaibe, 2008), the effects of rainfall and discharge also need to be considered (Gbeyetin, 2014). Moreover, when carrying out a vulnerability assessment in the lower Mono basin, Kissi (2014) underscored the evidence of changes in the patterns of precipitation and river discharge over the period 1971-2010; she noted the recurrence of flooding (high, moderate and low magnitude), and concluded that the return period of flood events such as that of 2010 (high magnitude) is around five (5) years. Ntajal et al., (2016b) also argued that the lower Mono River basin – Lacs district, Togo– will mostly experience floods of 2-year 5-year frequency. In addition, “all districts in the lower Mono River basin are vulnerable to flooding” (Ntajal et al, 2016a p1561).

On assessing rainfall trend in Mono watershed, Ntajal et al., (2016b) noted that over the period 1961-2013, there is a significant decreasing trend in rainfall at the station of Sokode (upstream), while an insignificant increase in rainfall is observed in the downstream (Atakpame, Sotouboua, Aklakou and Tabligbo). The same assessment was conducted by Amoussou (2010) on the period 1961-2000 using a cubic spatial interpolation for rainfall data in the watershed. The results showed an overall decreasing trend of rainfall. In a further study, the same author used kriging for interpolating rainfall data on the period 1988-2010 and observed a significant increase in the intensity of the maximum daily rainfall (Amoussou et al., 2014). It is worth noting that previous studies have accounted for the spatial variability of climate in Mono watershed (Rossi and Blivi, 1995; Klassou 1996; Ago et al.2005; Amoussou, 2010; Gbeyetin, 2014)

2.3. Future Climate Data and Bias Correction

Basically, the analysis of climate change impact on river flow over a forthcoming period requires climate projection data provided by climate models. These projections are based on future emission scenarios. Over the years, new sets of emission scenarios are released. In 1992, the IS92 scenarios were presented by the Intergovernmental Panel on Climate Change (IPCC). Latter, in 2000 the Special Report on Emission Scenarios (SRES) were released and recently, the Representative Concentration Pathways (RCP) were published and served as scientific basis for the fifth assessment report of IPCC (AR5). RCPs are a consistent set of scenarios developed under the Coupled Model Inter-comparison Project Phase 5 (CMIP5). They include time series of

emissions and concentrations of the full suite of greenhouse gases and aerosols and chemically active gases, as well as land use/land cover (Moss et al., 2010). RCPs are meant to serve as input for climate modelling as well as for the assessment of mitigation options (Vuuren et al., 2011). There are four RCPs named according to the associated radiative forcing in 2100 with respect to the year 1850. These are: RCP2.6 (radiative forcing reaches approximately $2.6\text{W}/\text{m}^2$ before 2100 and declines); RCP4.5 and RCP6.0 (intermediate pathways in which radiative forcing stabilizes at $4.5\text{W}/\text{m}^2$ by 2100 and peaks after 2100 at approximately $6\text{W}/\text{m}^2$, respectively); and, finally the high pathway RCP8.5 (radiative forcing exceeds $8.5\text{W}/\text{m}^2$ by 2100 and keep increasing for a while) (Moss et al., 2008).

But using raw projections from climate models — global climate models (GCMs) and regional climate models (RCMs) — when conducting climate change impact studies is problematic because of the significant biases introduced by the models. Those biases include systematic model errors caused by imperfect conceptualization and spatial averaging within grid cells (Teutschbein and Seibert, 2012). Although RCMs have finer spatial resolution (25-50 km) than GCMs (100-250 km), they also have to be handled with caution (Christensen et al., 2008; Varis et al., 2004).

To comply with that school of thought, several researchers have investigated various bias correction methods. The methods may vary according to the climate variable one is willing to correct. Teirink et al. (2009) used shifting and scaling in correcting temperature, and a powered transformation for daily precipitation data over the Rhine basin (western Europe). The correction was applied to RCM REMO climate data — already downscaled to a resolution of 0.088° — and yield good results. In the same context, Teutschbein and Seibert (2012) applied 5 different methods for precipitation and 4 for temperature data extracted from 11 RCMs in Sweden. The local intensity correction (LOCI), power transformation, linear scaling, distribution mapping and delta-change were applied to precipitation on one hand, and on the other hand, temperature was corrected with the last three methods in addition to the variance scaling. The results showed that all bias correction methods which were performed have improved raw data from the RCMs. Furthermore, at the regional level, bias correction of RCM climate variable has been undertaken as well, and some instances are hereafter described. In the Niger river basin (West-Africa), Oyerinde (2016) used quantile mapping for precipitation and delta-change for temperature data from 8 RCMs, and concluded the methods as suitable for improving the data. But Mbaye (2015) applied a method based on fitted histogram equalization for correcting both temperature and rainfall data from the RCM REMO in the Senegal basin. Again, satisfactory results were found.

In the Ouémé basin (Benin), N'Tcha M'po et al., (2017) investigated the linear scaling, the delta approach and the quantile mapping methods for correcting precipitation data from 4 RCMs and stated that empirical and adjusted quantile mapping are the most effective.

2.4. Assessment of Climate Change Impact on River's Discharge

Considering the importance of river flow in watershed management, many researchers have embarked on modelling and projecting rivers' discharge. Carrying out such studies in the current context of climate change and variability is of high importance (Roudier et al., 2014). Therefore, including climate scenarios and projections into hydrological modelling has become critical for assessing the risks and impacts arising from climate change. Various types of hydrological models can be distinguished – e.g. physically-based, conceptual, lumped, semi-distributed and distributed. Physically based models are built on a logical and flexible structure which is similar to the real-world system. In such models, processes are described by detailed physical equations (Lundin et al., 2000). But, conceptual models operate with highly simplified form of physical laws that describe relationship between input variables and outputs (Gayathri et al., 2015). As for lumped, semi-distributed and distributed models, they refer to a spatial consideration of the watershed. The first one considers the basin as a homogenous whole; the second one takes into account flow contribution from various sub-basins and treat each as a homogenous system; whereas the last one divides catchments into several cells or grids which drain water flow through the basin (Xu, 2002).

All over the world, several studies related to climate change impact on river's discharge have been conducted. Some instances of such studies are presented in the Table 1.

Table1: Instances of studies related to climate change impact on river's runoff

Author	Watershed/ Country	Climate scenario	Climate model	Hydrological model	conclusion
Xu and Luo, 2015	River Huangfuchuan and River Xiangxi (China)	SRES A1B	UKMO HadCM3, UKMO HadGEM1, NCAR CCSM3.0, MPI ECHAM5, IPSL CM4, CSIRO MK3.0, and CCCma CGCM3.1	SWAT	Satisfactory performance of SWAT model
Babur et al., 2016	Mangla Basin (Pakistan)	RCP4.5 RCP8.5	BCC-CSM 1.1-m; CCSM4; CSIRO BOM ACCESS1-0; GFDL-CM3, MIROC5, MRI-CGCM3, and UKMO-HadGEM2	SWAT	Flows at different stations are well simulated
Driessen et al., 2010	Ourthe catchment, Belgium (Luxembourg)	SRES A1B, A2 and B1	ECHAM5/MPIOM downscaled with REMO	HBV-light	HBV model performs quite well in simulating mean streamflow
Kebede, Diekkrüger, and Moges, 2014	Sore watershed, (Ethiopia)	A1B and B1	REMO CGCM3.1	WaSiM-ETH HBV-Light	Both the hydrological and climate models were consistent concerning the overall direction of change, regardless of magnitude
Mbaye et al., 2015	Upper Senegal basin (Senegal)	RCP4.5 RCP8.5	REMO	MPI-HM	Good simulation of river flow
Biao; 2017	Ouémé River Basin	RCP4.5 RCP8.5	HIRHAM5 and RCA4	HyMoLAP	HyMoLAP is suitable for modelling river discharge in the Ouémé River basin

2.5. Hydrological modelling and Assessment of Climate Change Impact in Mono River watershed

Amoussou (2010) found that GR2M model is good for simulating the discharge in the Mono basin under the condition of negligible influence from the Nangbeto dam. This result confirms the suggestion of Paturel et al. (2006) to neglect the influence of dam when analysing the flows of a watershed. Furthermore, the hydrological model GR4J showed good simulation only in calibration

period (Amoussou, 2015) whereas the GRP model performed quite better (Amoussou et al., 2015). Furthermore, Trambly et al. (2014) has assessed flood risk in Mono River basin using soil saturation as flood generating process, and an ensemble of four regional climate models – REMO, RegCM, HadRM3 and RCA – under SRES A1B.

Unfortunately, most flood-related studies in Mono River, so far, have not considered discharge projection with respect to climate scenarios. But, assessing flood risks using the latest set of climate scenarios (RCPs) and widening the array of possible future taking into account more than one scenario – e.g. RCP4.5 and RCP8.5 – will provide much more scientific information to support mitigation and adaptation strategies.

CHAPTER III: MATERIAL AND METHODS

3.1. The Study Area

The Mono watershed occupies an area of 27,822 km² shared between Togo and Benin. Specifically, it is located between the latitudes 06°16' and 09°20'N, and the longitudes 0°42' and 2°25'E (Figure 1). It hosts the Nangbeto hydroelectric dam constructed in 1987. The major part of the basin lies in Togo territory with 21,750 km² while that of Benin stretches on 6,072 km² (Figure 2). The river serves as natural border between the two countries. The main tributaries of the Mono River are Anié (161 km), Amou (114 km), Amoutchou (62 km), Kra (69 km) and Ogou (207 km). The climate is subequatorial (two rainy seasons and two dry seasons) downstream and tropical (one rainy seasons and one dry season) upstream. In the subequatorial regions where rainfall peak is reached in August, mean annual rainfall amounts 1230 mm. But tropical regions which are closer to the coast experience first rainfall peak in June and a second one in September, with mean annual rainfall of 1068 mm.

This study focuses on the town of Athiémé which is located in the south-western part of Benin and within Mono watershed (Figure 2). It covers an area of 238 Km² and shares borders with the towns of Lokossa in the north, Grand-Popo in the south, Houeyogbé in the Est and the Republic of Togo in the west. Athiémé has a population of 56,483 inhabitants along with a population density of 246 hab/Km² (2015's population census). Within the decade 2002-2013 the population growth rate has almost doubled going from 1.8% to 3.2% in 2013. The climate in Athiémé is subequatorial with a bimodal rainfall regime and the mean annual rainfall within the period 1997-2011 is 939.5 mm. Furthermore, the main economic activities in Athiémé are agriculture and fisheries. Actually, 78% of the land is devoted to agriculture.

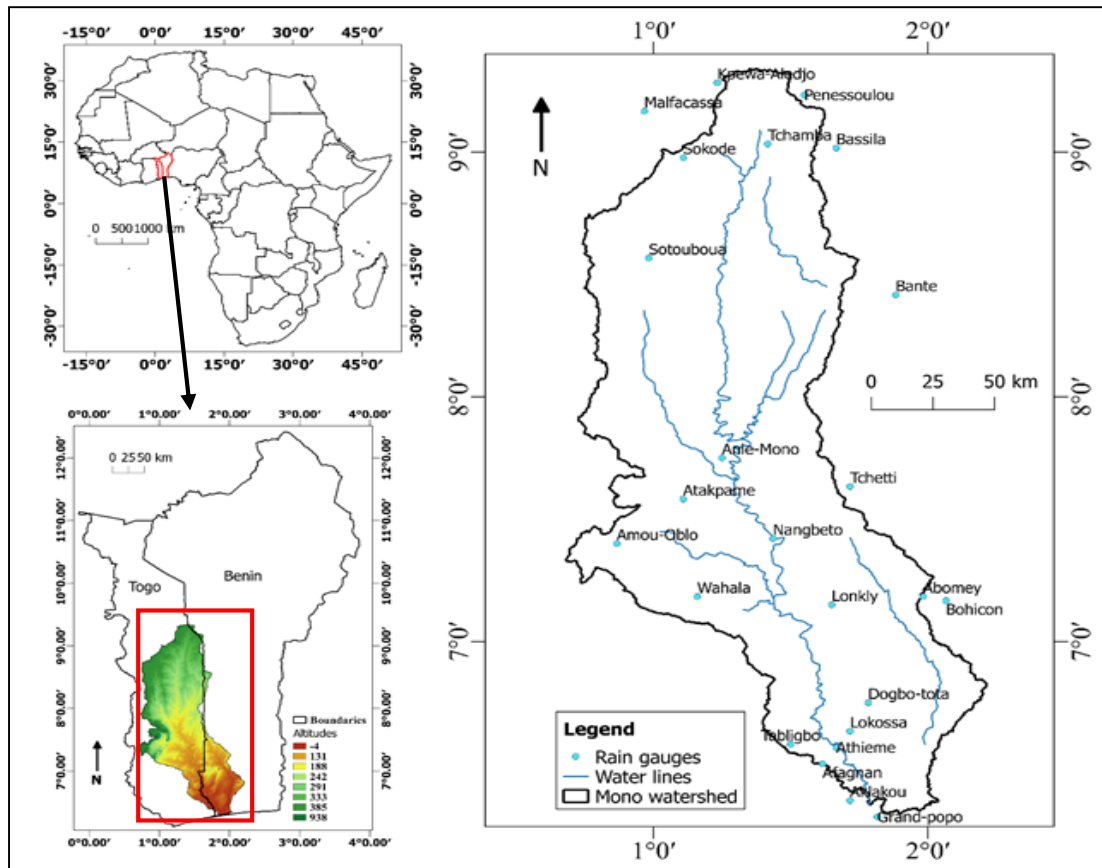


Figure 1.1: Location of Mono watershed

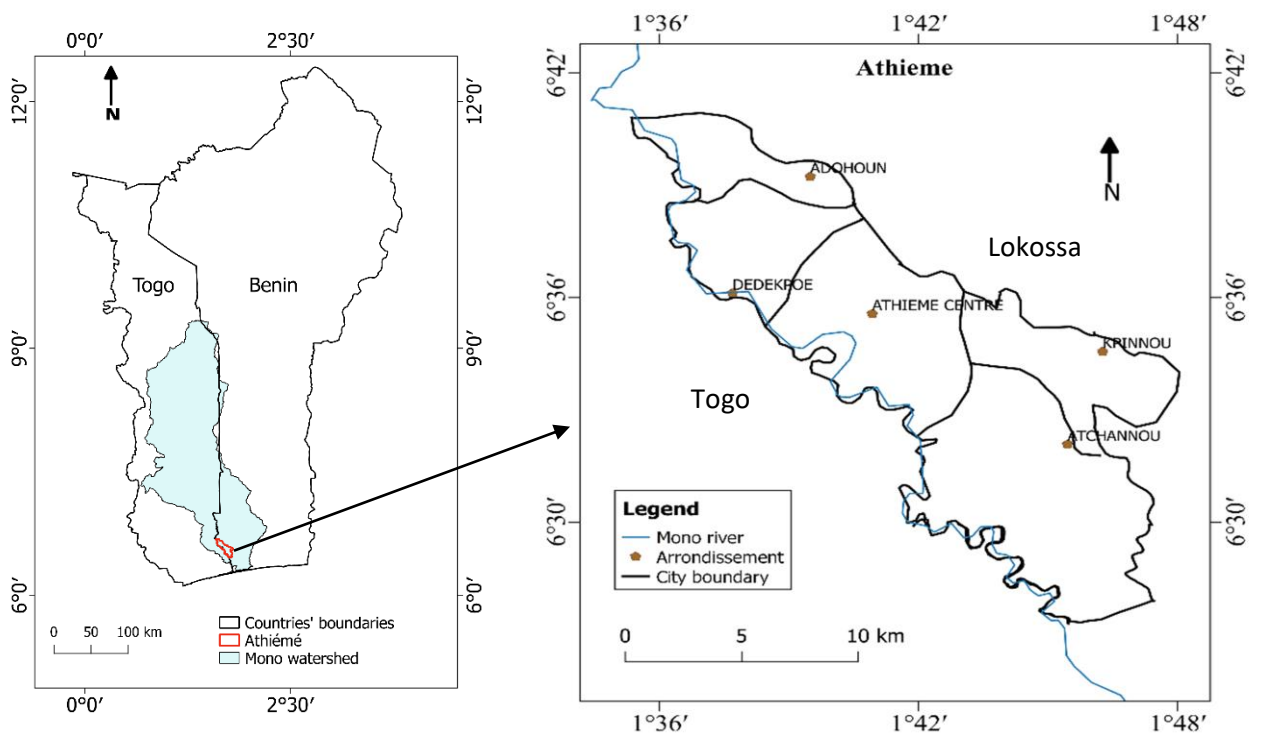


Figure 1.2: Location of Athiémé

3.2. Methods

This section presents the methods that are used to attain each research objective.

3.2.1. Analysis of Past and Future Climate Trend

Rainfall analysis

In order to assess the trend of rainfall at the watershed scale, and because rainfall data is not measured in every single grid of the watershed, spatial interpolation was required. In the scope of this study, kriging interpolation method was chosen over other methods — such as arithmetic mean, Thiessen polygon, inverse distance weighting — because (i) it takes into account not only the distance between observation stations and estimation point, but also the distance between stations taken two by two, (ii) it is a stochastic method which provides the best linear unbiased predictions, (iii) the interpolation error can be estimated. Nonetheless, one of the limitations of kriging is that it is not suitable when there are few observation points.

Kriging was basically developed for geostatistics purposes (Matheron, 1963) but is widely used in climatology. Among the various types of kriging, the ordinary kriging (OK) which assumes that the user has no information on the mean of the process being studied, was used. It is worth noting that the ‘backbone’ of kriging is the variogram which explains the variance of the studied variable with respect to distance between observation points. Equation 1 presents the formula of variogram.

$$\gamma(h) = \frac{1}{2N(h)} \sum_{i=1}^{N(h)} (z(p_i) - z(p_i + h))^2 \quad (1)$$

where $\gamma(h)$ is the variogram, $N(h)$ the number of couple of points separated by the distance h , $z(P_i)$ the observed rainfall at location P_i , and $z(P_i + h)$ the observed rainfall at location $P_i + h$.

The variogram is then modeled with the appropriate function or theoretical variogram (Figure 3). For rainfall data, the spherical, exponential and Gaussian models are commonly used (Muhamad Ali and Othman, 2016; van de Beek et al. 2011; Verworn and Haberlandt, 2011; Ly et al., 2011; Lawin, 2007; Baillargeon, 2005).

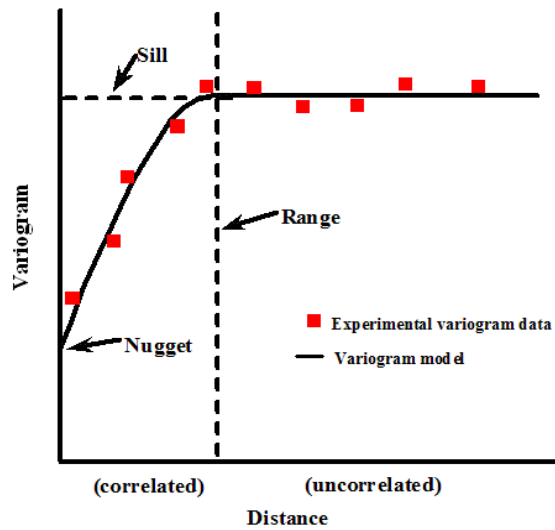


Figure 3: Components of a variogram

Source : https://vsp.pnnl.gov/help/vsample/Kriging_Variogram_Model.htm

Samples of spherical, exponential and Gaussian models are presented by Figure 4. The next step is then to identify among these three models the suitable one.

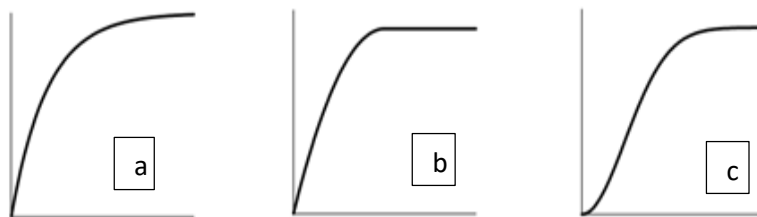


Figure 4: Variogram models (a) exponential, (b) spherical, (c) gaussian

The choice was first of all guided by the characteristics of the experimental variogram –computed with equation (1). Exponential and spherical models were chosen over the gaussian because the latest start with a parabolic curve whereas the two others have a linear beginning as for in this study.

The spherical model is given by

$$\gamma(h) = \begin{cases} C_0 + C \left(\frac{1}{3} \frac{h}{a} - \frac{1}{2} \frac{h^3}{a^3} \right) & \text{if } 0 < h < a \\ C_0 + C & \text{if } h \geq a \end{cases} \quad (2)$$

and the exponential model is given by

$$\gamma(h) = C_0 + C \left(1 - \exp \left[3 \left(\frac{h}{a} \right)^2 \right] \right) \quad (3)$$

where C_0 is the nugget, C the sill and a the range.

Finally, deciding whether an experimental variogram should be fitted with the exponential or the spherical one could be done either manually — on a graphical basis — or automatically. Automatic fitting implies using an objective function to assess how well the theoretical model matches the experimental one. This approach was adopted in this study using the Nash-Sutcliffe efficiency coefficient (Nash and Sutcliffe, 1970) NSE as objective function (Equation 4).

$$NSE = 1 - \frac{\sum_{i=1}^N (V_{ex}^i - Q_{th}^i)^2}{\sum_{i=1}^N (V_{ex}^i - \overline{V_{ex}})^2} \quad (4)$$

where, V_{ex}^i , V_{th}^i , Q_{ex} and N are respectively the experimental variogram of year i , theoretical variogram of year i , average of experimental variograms and the length of the study period.

More explicitly, the following steps were implemented: (i) computation of daily variograms using identical lag distances for each year; (ii) for each year, the mean variogram which is the arithmetic mean of daily ones is computed with respect to lag distances; (iii) the mean variogram are adjusted with both spherical and exponential models; (iv) computation of Nash coefficient for both models in order to identify the best one —the one with highest Nash coefficient; (v) for each year, daily rainfall data are interpolated with kriging, using the best theoretical model identified and a grid cell of 0.0045x0.0045 degree corresponding to 0.5 km x 0.5 km. Thus, the interpolated rainfall in each grid is averaged to watershed scale to get the mean areal rainfall.

Temperature analysis

Within the watershed and for the study period, temperature data are provided only by the stations of Tabligbo, Atakpame and Sokode (see Figure 1). Thus, kriging cannot be envisaged as for rainfall data. On trying to get average temperature using Thiessen polygons, the result was not usable because the longitudes of the three stations are very close. Thus the polygons generated were too slim and do not cover the entire watershed. Finally, the arithmetic mean of the three stations were taken as the one of the watershed.

3.2.2. Projected Climate Data and Bias Correction

Raw outputs from regional climate models (RCM) must be corrected prior to local impact studies because of the bias they encompass (Sylwia Trzaska and Emilie Schnarr, 2014). There are several bias correction methods but in this study, the methods of delta, linear scaling and empirical quantile mapping (EQM) are used because they have produced satisfactory results in previous studies (N'Tcha M'Po et al. 2017; Obada et al. 2017; Bontogho, 2015). The delta method corrects biases in the mean and is applicable to any kind of climate variable. But it does not remove biases in the coefficient of variance (Xu, 2017). The linear scaling method aims to perfectly match the mean of corrected values with that of observed ones and operates on a monthly basis (Fang et al. 2015; Linderink et al., 2001). This method consists of scaling the simulation with the difference (additive scaling) or the quotient (multiplicative scaling) between the observed and simulated means (Wetterhall, 2012). Additive scaling is preferably applied to temperature and the multiplicative one to precipitation (Xu, 2017). As for the empirical quantile mapping (EQM) it uses the cumulative distribution function (CDF) and is applicable to any kind of climate variable. The results of N'Tcha M'Po et al. (2017), Essou and Brissette (2013) and Speth et al (2010), who bias-corrected REMO data in the Ouémé watershed (Benin), guided the choice of correction methods in this study. Rainfall was corrected with delta method in the south, multiplicative scaling in the central part and EQM in the north. As for temperature data, they were corrected using only EQM. Equations 5, 6 and 7 presents the formula of delta, multiplicative scaling and EQM respectively.

$$P_{cor,d} = P_{raw,d} \times \frac{\overline{P_{obs}}}{\overline{P_{RCM}}} \quad (5)$$

where $P_{cor,d}$ and $P_{raw,d}$ are the corrected and uncorrected rainfall of dth day; $\overline{P_{obs}}$ and $\overline{P_{RCM}}$ are the mean values of daily observed and simulated rainfall.

$$P_{cor,m,d} = P_{raw,m,d} \times \frac{\overline{P_{obs,m}}}{\overline{P_{raw,m}}} \quad (6)$$

where, $P_{cor,m,d}$ and $P_{raw,m,d}$ are corrected and uncorrected rainfall on dth day of mth month; $\overline{P_{obs,m}}$ and $\overline{P_{raw,m}}$ are the mean values of daily observed and simulated data of mth month.

$$y = F_{obs}^{-1}(F_{RCM}(x)) \quad (7)$$

y is the corrected rainfall, x the value of rainfall to be corrected; F_{obs}^{-1} the inverse of the CDF of observed rainfall and F_{RCM} the CDF of data simulated by the RCM.

3.2.3. Hydrological Modelling and Discharge Projection

General Presentation of the Hydrological Model HBV-light

Hydrological modelling in this study is carried out using HBV-light (Hydrologiska Byråns Vattenbalansavdelning, Seibert and Vis (2012)). Its input data are the areal precipitation, temperature, potential evapotranspiration and observed discharge. HBV is part of IHMS (Integrated Hydrological Modelling System) and is used for hydrological prediction, discharge simulation, as well as flood analysis under climate change. The versions of the model vary according to the purpose. In this study, the HBV-Light-GUI, version 4.0.06 was used. It has many characteristics among which the following ones could be mentioned: (i) simple structure, (ii) conceptual, (iii) lumped, (iv) requires moderate amount of input data, and (v) not computationally expensive.

The use of HBV in Benin is not new. In the framework of the Impetus project, Bormann and Diekkrüger (2003) used the HBV (Bergstrom, 1995) model for discharge prediction over the Upper Ouémé Basin. The model has also been applied in Mékrou Basin and was found adequate for the simulation of the various parts of the hydrograph during the period 2004-2011 (Gaba et al., 2015). In the Benin portion of Niger River Basin, HBV-light was used to assess the impact of climate change on blue and green water (Badou, 2016).

Figure 5 shows the structure of HBV-light.

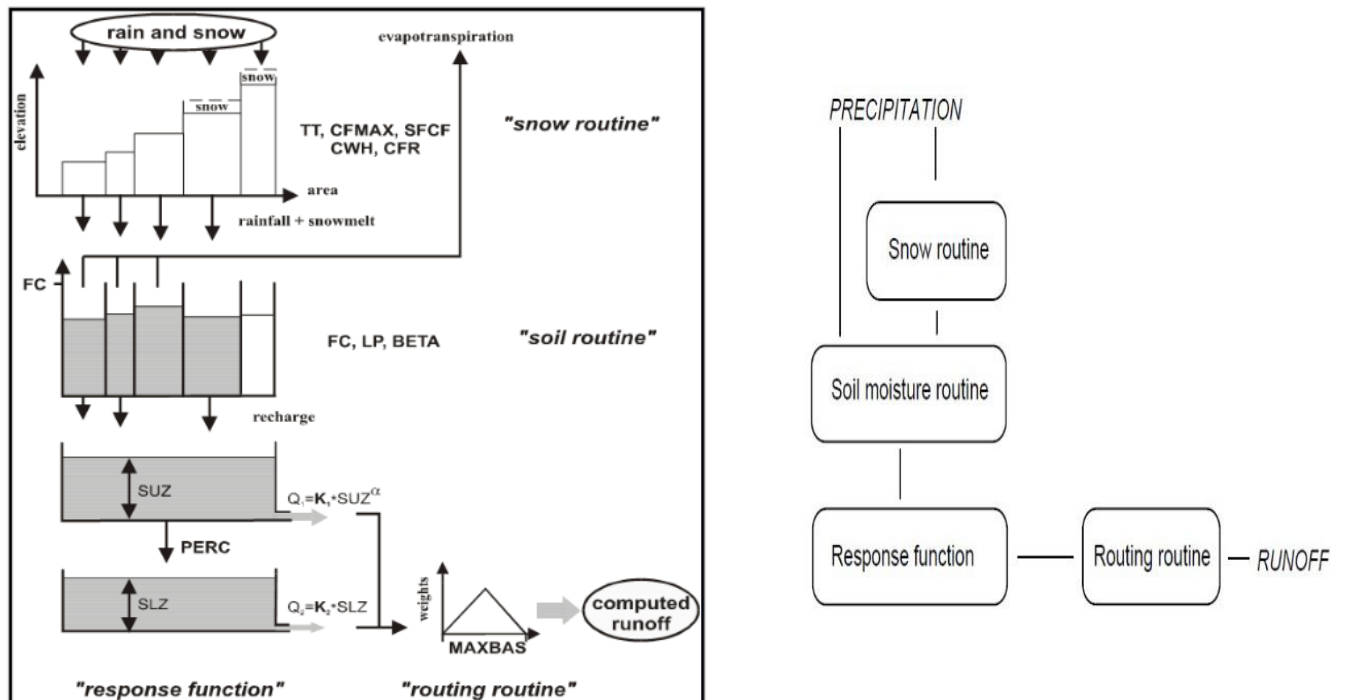


Figure 5: General structure of HBV-light model

HBV-light is organized into four (4) sub-models which deal with different aspects of water balance. Those submodels are: the snow routine, the soil routine, the response function and the routing routine. The input data, output data and parameter of each of them is summarized in Table 2.

Table 2: Sub-models of HBV-light

Sub-model	Input data	Output data	Parameter
Snow routine	Precipitation Temperature	Snow pack, snow-melt	TT = threshold temperature ($^{\circ}C$) $CFMAX$ = degree- Δt factor ($mm\ ^{\circ}C^{-1}\ \Delta t^{-1}$) $SFCF$ = snowfall correction factor (-) CFR = refreezing coefficient (-) CWH = water holding capacity (-)
Soil Routine	Potential evapotranspiration; Precipitation; Snowmelt	Actual evapotranspiration; Soil moisture; Groundwater recharge	FC = maximum soil moisture storage (mm) LP = soil moisture value above which AET reaches PET (mm) $BETA$ = parameter that determines the relative contribution to runoff from rain or snowmelt (-)

Response function	Groundwater recharge ; Potential evapotranspiration	Runoff; Groundwater level	PERC = threshold parameter (mm Δt^{-1}) Alpha = non-linearity coefficient (-) UZL = threshold parameter (mm) K = storage (or recession) coefficient (Δt^{-1})
Routing routine	Runoff	Simulated runoff	MAXBAS = Length of triangular weighting function (Δt)

The response function is built upon a single linear reservoir model where the runoff $Q(t)$ at time t is supposed to be proportional to the water storage $S(t)$.

$$Q(t) = K \times S(t) \quad (8)$$

$$S(t) = SP + SM + S_{UZ} + S_{LZ} + Lakes \quad (9)$$

where SP is the snow pack, SM the soil moisture, S_{UZ} upper groundwater zone, S_{LZ} lower groundwater zone and $Lakes$ the volume of lakes.

The water balance of the catchment is given by:

$$P(t) = E(t) + Q(t) + \frac{dS(t)}{dt} \quad (10)$$

The general structure of HBV-light, considers the soil as divided into two boxes, the upper groundwater zone S_{UZ} , and the lower groundwater zone S_{LZ} , and the flow from groundwater boxes, $Q_{WG}(t)$ is:

$$Q_{GW}(t) = K_2 \cdot S_{LZ} + K_1 \cdot S_{UZ} + K_0 \cdot \max(S_{UZ} - UZL, 0) \quad (11)$$

where S_{LZ} is the recharge added to the lower groundwater box, S_{UZ} the recharge added to the upper groundwater box, UZL a threshold parameter, K_0 , K_1 , K_2 the storage (or recession) coefficient.

Then, the simulated streamflow, Q_{sim} , is obtained by applying a triangular weighting function defined by the parameter $MAXBAS$.

$$Q_{sim}(t) = \sum_{i=1}^{MAXBAS} c(i) \cdot Q_{GW}(t - i + 1) \quad (12)$$

$$\text{Where } c(i) = \int_{i-1}^i \frac{2}{MAXBAS} - \left| u - \frac{MAXBAS}{2} \right| \cdot \frac{4}{MAXBAS^2} du. \quad (13)$$

Sensitivity Analysis

Sensitivity analysis is very important when carrying out hydrological modelling. Its main objective is to identify parameters which are “sensitive” to change. In other words, parameters for which a slight change can induce remarkable change in the model’s outputs. In this thesis, the method used to conduct sensitivity analysis consists of computing R^2 for series of NSE and each parameter. The series of Nash coefficient and corresponding parameter sets were generated using the genetic calibration algorithm GAP.

Model Calibration and Validation

Because of the high level of missing values in discharge time series, eight (8) years have been used for calibration and validation. Only years without missing data during the rainy season (April-November) were considered. These are: 1985, 1988, 1989, 1990, 1991, 1992, 1998 and 2010. The calibration period covers 1988-1992 whereas validation is done on years 1985, 1998 and 2010. The period 1988-1992 is used for calibration because it accounts for high discharge years (1988, 1989, and 1990) and low ones (1989 and 1992). As for validation which is done on independent years, it takes into account the period before the construction of the Nangbeto Dam (1985) and period after building of the dam (1998, 2010). The objective function used during the calibration is the NSE (see section 3.3.2.2.). The principle consists of varying the parameters till a relatively good efficiency coefficient is obtained for the calibration period. Then these “good” parameters are used for validation and afterward for the future periods. In the present study, HBV-light was automatically calibrated using the genetic calibration algorithm GAP embedded in the model. As shown by Table 3, HBV-light has 13 parameters but only 8 are taken into consideration in this study, because the remaining five govern the snow routine and are not relevant for the study area.

3.2.4. Assessment of the Impacts of Projected Discharges on Human Security

To assess the potential impacts of projected discharges on human security, use was made of digital elevation model (DEM), values of water height at Athiémé and land use/land cover maps 1981 and 2015 of Mono watershed and Athiémé. All areas in Athiémé’s town, having their elevation lower than the projected water height were considered as susceptible to be flooded. Then the areas of susceptible and non-susceptible places are computed. This method assumes that elevation will not vary significantly until 2050. In addition, years 2010 and 1983 are respectively taken as reference for high and low flow. In fact, 1983 was one the driest years recorded in Mono watershed during the last 40 years, especially in its southern part (Klassou, 1996; Amoussou, 2010). The year 1983 was also characterized by low average and maximum discharge, 28.3 m³/s and 177 m³/s

respectively. In addition, the drought of 1983 triggered tremendous deficit in terms of agricultural production and water availability. On the other side, 2010's flood event was one of the most disastrous in Athiémé, as earlier described in section 1.1. More explicitly, the projected maximum discharges will be compared to those of years 1983 and 2010, in order to have an idea of the potential damage one might expect in the future.

3.3. Data Collection and Analysis

3.3.1. Data Collection

In order to achieve the objectives of this study both secondary and primary data were used. They include hydroclimatic and geographical data.

Observed Hydroclimatic Data

Daily observed rainfall, temperature and evapotranspiration were collected from meteorological institutes of Benin and Togo (DMN, Direction de la Météorologie Nationale) for the period 1981-2010 (Table 4). The period 1981-2010 is the current normal used for climatological analysis and this study aims at taking it into account, as previous studies have already accounted for other normals (Amoussou, 2010; Kissi, 2014; Ntajal, 2016b). Rainfall data were collected at 24 rain gauges within and around Mono watershed (not farther than 25 km). In fact, during the interpolation process, the selected rain gauges which are not within the watershed were useful when nearer ones which are in lack data. Indeed, when a station lacks data on a given day, it is not used for the variogram computation of that specific day but will still be useful for days it has data for. That is why no rain gauge was excluded because of missing data.

Temperature data were collected for the three synoptic stations which are in the watershed (Tabligbo, Atakpamé and Sokodé).

As for evapotranspiration (ETP), data from Atakpamé station were taken into consideration. Actually, the World Meteorological Organization, recommends a density of one per 50,000 km² for evapotranspiration measurement network (WMO, 1996 cited by Oudin 2004). It buttresses the choice of only one station for ETP considering the fact that Mono watershed covers an area of 27,822 km² (which is less than 50,000 km²). In addition, Oudin (2004) —while assessing the relevance of different ETP computation methods to rainfall-runoff hydrological models— defined his ideal ETP station as the one being not farther than 100 km to the centroid of the assessed

watershed. The station of Atakpamé located 38 km away from Mono watershed's centroid fulfilled this condition, unlike Tabligbo and Sokodé stations which are respectively 135.4 km and 135.6 km distant to the centroid. It is worth mentioning that ETP data collected from the meteorological institute of Togo were computed using Hargreave-Samani's formula (Hargreave and Samani, 1985) which requires only minimum and maximum temperature.

Furthermore, daily discharge data at Athiémé station were provided by Benin Water Directorate (DGEau, Direction Générale de l'Eau). These data include substantial missing values (36%) within the study period 1981-2010. Especially, for years 1995 and 2001 observation data are not available. But, for the sake of analysing the trend of Mono river maximum discharge at Athiémé, data of those two years were imputed using daily average of the two contiguous years on either side of the missing year (1993, 1994, 1996, 1997 for 1995; and 1999, 2000, 2002, 2003 for 2001).

Future Climate Data

In the framework of this study, the regional climate model REMO, version REMO2009 is used at horizon 2050 and under the representative concentration pathways RCP4.5 and RCP8.5. The climate variable extracted are rainfall and precipitation for the period 1981-2050.

Table3: Characteristics of REMO2009

Model name	Institution	Driving model
REMO2009	Helmholtz-Zentrum Geesthacht, Climate Service Center, Max Planck Institute for Meteorology	Max Planck Institute - Earth System Model running on low resolution grid (MPI-ESMLR)

This choice was guided by three main reasons. First of all, Previous studies have reported the adequacy of REMO for climate change impact analysis over West Africa. Akinsanola et al. (2015) noticed that REMO fairly simulates rainfall in West Africa and concluded that it can be used for future climate projections in the region. Secondly, horizon 2050 represents the milestone for many regional and international projects. In addition, projecting climate to 2050 is preferable because in this study the farther the projection, the higher the uncertainty in the inferences made for human security and infrastructures (see section 3.2.4). Finally, RCP4.5 and RCP8.5 are chosen based on their relevance to the countries. Actually, RCP4.5 has already been used in the national communications of Benin and Togo as well and RCP8.5 expresses the path for worst climate conditions. RCP2.6 is recommended for high emitting countries and RCP6.0 as high average condition is not available for our region.

Geographical data

First of all, Digital Elevation Model (DEM) from Shuttle Radar Topography Mission was downloaded at a resolution of 30 arc seconds (SRTM30). In fact, Amoussou (2010) has already used the same data when conducting spatial interpolation of climatic data over Mono watershed.

Secondly, coordinates of community infrastructures within Athiémé districts were collected through field work. The targeted infrastructures include schools, health centres, religious places (mosques, churches and convents), markets, public places (where community meetings hold), plants (factories), police stations, town and districts halls, post office, and bridges. 61 villages were covered and information on geographical coordinates — longitude, latitude and elevation — were collected using a geographical positioning system (GPS) receiver.

Table 4: Summary of Data Collected and used in this study

Data	Period	Relevance	Source
daily air temperature	1981-2010	Trend analysis and input for hydrological modelling	DMN Benin and Togo
daily rainfall	1981-2010	Trend analysis and input for hydrological modelling	DMN Benin and Togo
daily potential evapotranspiration	1981-2010	Trend analysis and input for hydrological modelling	DMN Benin and Togo
Daily discharge	1981-2010	Assessment of the performance of hydrological model	DGEau Benin
REMO climate data	1981-2050	Trend analysis and input for hydrological modelling	CORDEX database
DEM of SRTM30	---	Assessment of the impact of projected discharges on infrastructures	Online https://earthexplorer.usgs.gov/
Land use/land cover maps	1980,2015	Assessment of the impact of projected discharges on infrastructures	CENATEL

Coordinates of communities' infrastructures within Athiémé	---	Ground-truth of downloaded DEM; Assessment of the impact of projected discharges on infrastructures	Field work
--	-----	---	------------

3.3.2. Data Analysis

3.3.2.1. Trend Analysis

Rainfall and Temperature

Considering the fact that rainfall regime in Mono watershed is not homogenous, rainfall trend analysis is carried out with respect to three latitude-based regions as done in previous studies (Ntajal et al., 2016b; Amoussou, 2010). The regions are defined as follow: latitude < 7 ; $7 \leq \text{latitude} \leq 8$ and latitude > 8 . Hereinafter, these regions are respectively referred as southern part, central part and northern part of the Mono watershed. Analysis of past and future rainfall data took into account the following elements:

- Pattern of seasonal cycle of rainfall,
- Percentage of relative changes in the seasonal cycle, Homogeneity tests, namely Pettitt's and standard normal homogeneity (SNH) test on annual rainfall and annual mean temperature,
- Mann-Kendall test on annual rainfall and annual mean temperature, and
- Standardized Precipitation Index (SPI).

Percentage of relative changes in the seasonal cycle are computed using equation 14.

$$P_{c,m} = \frac{(R_{proj,m} - R_{norm,m})}{R_{norm,m}} \times 100 \quad (14)$$

Where, $P_{c,m}$, $R_{proj,m}$ and $R_{norm,m}$ are the percentage of change for m^{th} month, average projected rainfall of month m , and the average rainfall of month within the normal period.

In order to avoid bias introduced internally by REMO or by the correction methods used, percentage of relative changes are computed with respect to REMO's simulations for the period 1981-2005 –instead of observed data.

For both petitt's and SNH test, significance level $\alpha = 0.05$ and the hypotheses are set as follow:

- Ho: there is no change in yearly rainfall data;
- H1: there is a date at with there is a change in the data.

In addition, Mann-Kendall test is performed to point out whether there is a trend (increasing or decreasing) in the rainfall time series. It is done with confidence level of 95% and the hypothesis are:

- Ho: there is no trend is rainfall time series
- H1: there is a trend in rainfall time series.

Choosing a significance level $\alpha = 0.05$ means that if a test yields a p.value lower than 0.05, its null hypothesis Ho is rejected and the alternative one is accepted; but in case p.value is greater than 0.05, Ho is accepted and Ha is thus rejected.

Furthermore, the SPI (Mckee et al., 1993) is a tool recommended by the World Meteorological Organization (WMO) and widely used for quantifying precipitation deficit over different timescales (3 to 48 months). For the selected time scale, rainfall records are fitted with a probability distribution which is then transformed into a normal distribution so that the mean SPI for the location and desired period is zero. Hence, this method improves over the common anomaly method which do not take into account the fact that rainfall is typically not normally distributed for a cumulative period of 12 months or less. In the present study, the SPI 12 (for 12 months' timescale) is used in order to assess rainfall deficit or excess on a yearly basis. Moreover, SPI 12 is the one recommended for watershed analysis (WMO, 2012).

Table 5 presents the guideline for analysing SPI values (WMO, 2012, Mckee et al., 1993)

Table 5: SPI value range and corresponding interpretation

SPI value	Corresponding comment
2.0 and plus	Extremely wet
1.5 to 1.99	Very wet
1.0 to 1.49	Moderately wet
-0.99 to 0.99	Near normal
-1 to -1.49	Moderately dry
-1.5 to -1.99	Severely dry
-2 and less	Extremely dry

3.3.2.2. Goodness of fit

The outputs of HBV-light were assessed considering the goodness-of-fit criteria which includes the Nash-Sutcliffe efficiency, NSE (Nash and Sutcliffe, 1970), the percent bias PBIAS (Gupta et al., 1999) and the coefficient of determination R^2 . The NSE has been defined by Nash and Sutcliffe in 1970 as a coefficient which expresses the efficiency of the model regarding the proportion of the initial variance that it takes into account. It ranges from $-\infty$ to 1 with ideal value being 1.

$$NSE = 1 - \frac{\sum_{i=1}^N (Q_{obs}^i - Q_{sim}^i)^2}{\sum_{i=1}^N (Q_{obs}^i - \overline{Q_{obs}})^2} \quad (15)$$

where, Q_{obs}^i , Q_{sim}^i , $\overline{Q_{obs}}$ and N are respectively the observed flow, simulated flow, average observed flow and the length of flow time series.

The Percent bias (PBIAS) measures the average tendency of the simulated variable to be larger or smaller than the observed one. It ranges between $-\infty$ and $+\infty$ with the desired value being 0. A negative PBIAS implies model underestimation whereas a positive value indicates overestimation. But it is worth noting that it varies more during dry years than wet ones (Gupta et al., 1999)

$$PBIAS = \left[\frac{\sum_{i=1}^N (Q_{sim}^i - Q_{obs}^i)}{\sum_{i=1}^N (Q_{obs}^i)} \right] \times 100 \quad (16)$$

R^2 is a common and widely used criterion which describes the linear relationship between observed and simulated variable.

$$R^2 = \left[\frac{\sum_{i=1}^N (Q_{obs}^i - \overline{Q_{obs}}) \times (Q_{sim}^i - \overline{Q_{sim}})}{\sqrt{\sum_{i=1}^N (Q_{obs}^i - \overline{Q_{obs}})^2} \times \sqrt{\sum_{i=1}^N (Q_{sim}^i - \overline{Q_{sim}})^2}} \right]^2 \quad (17)$$

CHAPTER IV: RESULTS AND DISCUSSION

All the output results of data computing are presented, analysed and discussed in this chapter. The results are presented for each research objective.

4.1. Climate in the Mono Watershed

4.1.1. Observed Climate

4.1.1.1. Rainfall

Seasonal cycle varies from one part of the watershed to the other. The southern and northern parts are respectively characterised by bimodal and unimodal rainfall regime whereas, a transitory (not clearly bimodal neither unimodal) regime was found in the central region (figure 6). These results are in line with previous research findings (Amoussou, 2010 and Kissi, 2014, Ntajal et al., 2016b).

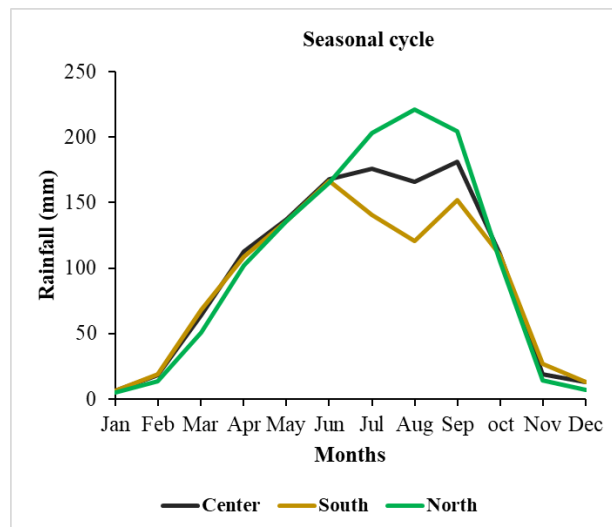


Figure 6: Rainfall seasonal cycles in Mono watershed

The results of Pettitt's and SNH tests performed on annual rainfall are summarized in Table 6 and those of Mann-Kendall test are in Table 7.

Table 6: Result of Pettit's and SNH test on observed rainfall

Region	Tests	Breakpoint	p.value	Conclusion
South	Pettitt	2001	0.0695	<i>There is no change in rainfall time series</i>
	SNH	2001	0.0497	<i>A change in rainfall time series occurred in 2001</i>
Centre	Pettitt	1987	0.3113	<i>There is no change in rainfall time series</i>
	SNH test	1983	0.0217	<i>A change in rainfall time series occurred in 1983</i>
North	Pettitt	1987	0.0952	<i>There is no change in rainfall time series</i>
	SNH test	1983	0.0025	<i>A change in rainfall time series occurred in 1983</i>

Table 7: Results of Mann-Kendall test performed on observed annual rainfall

Region	Tau	p.value	Conclusion
South	0.3977	0.0022	<i>Significant and increasing trend</i>
Centre	0.269	0.0385	<i>Significant and increasing trend</i>
North	0.2828	0.0295	<i>Significant and increasing trend</i>

Thus, rainfall in the three regions of Mono watershed had an increasing trend within the period 1981 to 2010.

Over the three parts of the watershed, Pettitt's test found no breakpoint, whereas SNH test detected a shift in south in 2001 and, in north and centre in 1983 (Figure 7).

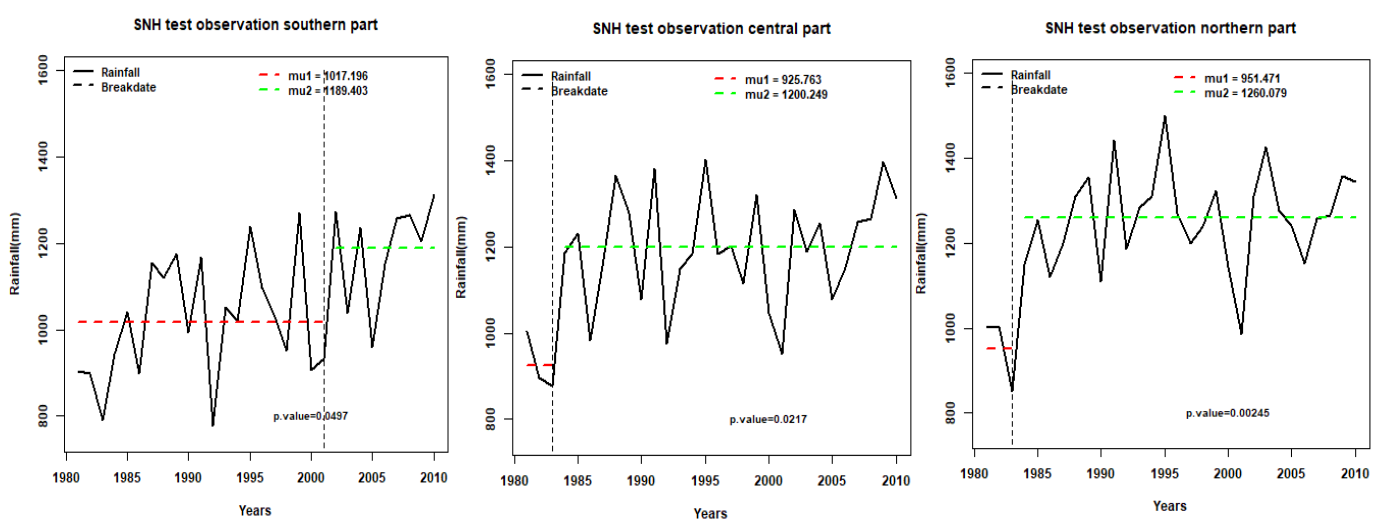


Figure 7: SNH test performed on observed annual rainfall time series in the south (left), centre (middle) and north (right)

In the southern part, although the two sub-periods demarcated by the breakpoint (1981-2001, 20 years and 2001-2010, 10 years) are lower than 30 years usually considered as normal in climatology analyses, the assumption of climate change cannot be formally rejected, considering the length of the time series used. In addition, the change noted in centre and north may be related to the well-known 1970 and 1980's drought which affected many West-African countries.

Furthermore, the results of the standardized precipitation index (SPI) computation are presented on Figure 8.

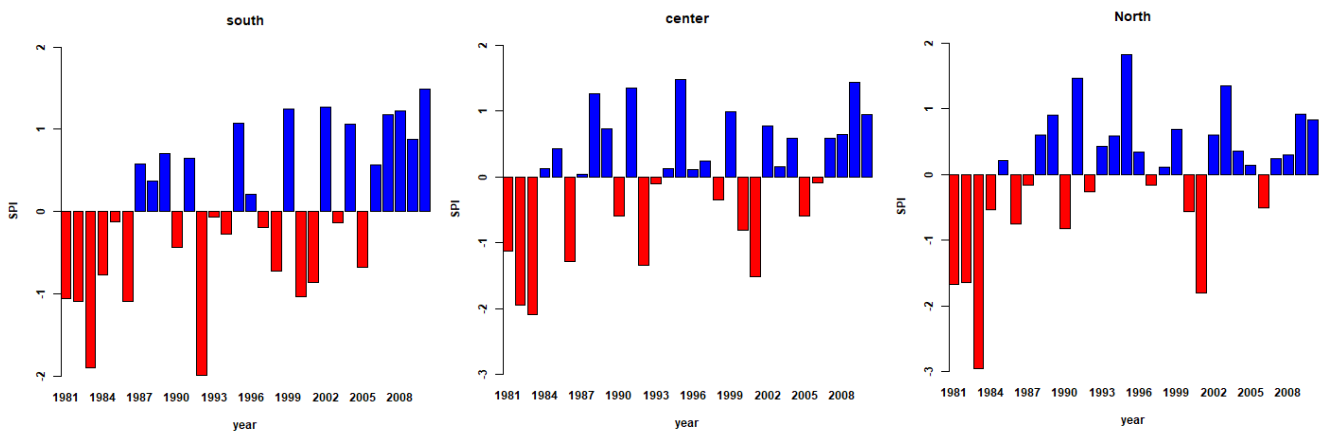


Figure 8: Standardized Precipitation Index (SPI) of observed annual rainfall in the south (left), centre (middle) and north (right)

The southern part recorded 16 dry years while the northern and central parts recorded 12. The longest dry period is 1981-1986 in the south, 1981-1983 in the central part and 1981-1984 in the north. In addition, the driest year is 1992 in the south (SPI = -1.99), and 1983 for both centre (SPI = -2.1) and north (SPI = -2.96). As of years of highest excess, it is 2010 in the south (SPI=1.49) and, 1995 in centre (SPI=1.47) and north (SPI=1.82).

4.1.1.2 Temperature

Homogeneity in temperature time series was assessed using Pettit's test and standardized homogeneity (SNH) test. Both tests reveal breakpoint in the time series of annual temperature (Figure 9).

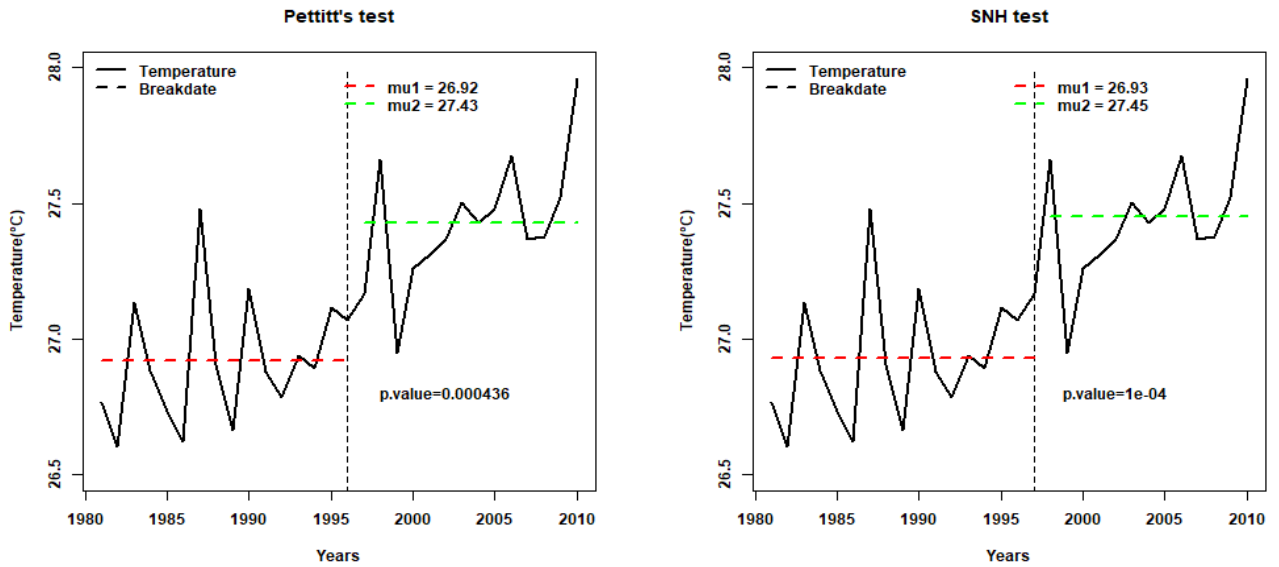


Figure 9: Pettitt’s test (left), Standardized Normal Homogeneity (SNH) test (right) for temperature

Pettitt’s test suggests that since 1996 mean annual temperature has increased by 0.51°C in Mono watershed compared to the period 1981-1995; whereas the results of SNH test implies an increase of 0.52°C from the period 1981-1996 to 1997-2010. In addition, Mann-Kendall test yields $p\text{-value} = 3.457 \cdot 10^{-6}$ and $\tau = 0.6$. Since $p\text{-value}$ is lower than α , the null hypothesis is rejected; meaning that there is a trend in the data set. As τ is positive, the trend is an increasing one. Moreover, anomalies are computed in order to identify years above and below normal (Figure 10).

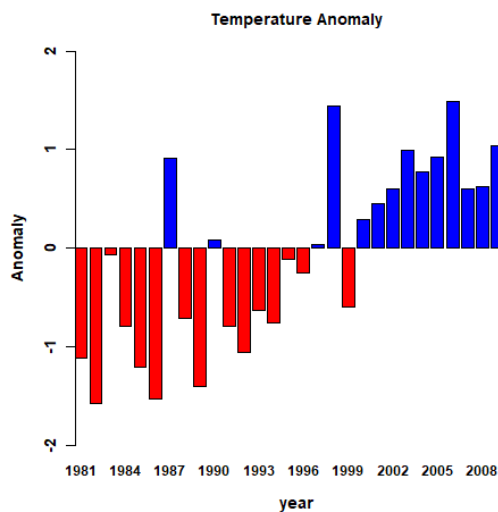


Figure 10: Anomaly of mean annual temperature over Mono watershed

From 1981 to 1997, temperature was globally below and near normal but since 1998 it has kept above the normal. It thereby corroborates the outputs from homogeneity tests. Moreover, these

results are in line with previous studies which noted similar increasing trend of temperature in West-Africa –Badjana, (2015) in the Kara river basin of Togo; Collins, (2011) over the West-African region.

4.1.1.3. Discharge

From 1981 to 2010, maximum discharge at Athiémé has varied between 90 m³/s and 951 m³/s with the lowest value recorded in 1994 and the highest in 1999 (Figure 11). However, Ntajal et al. (2016b) who found similar results, noted that the lowest maximum discharge occurred in 2009. This difference may be due to the gap filling methods used.

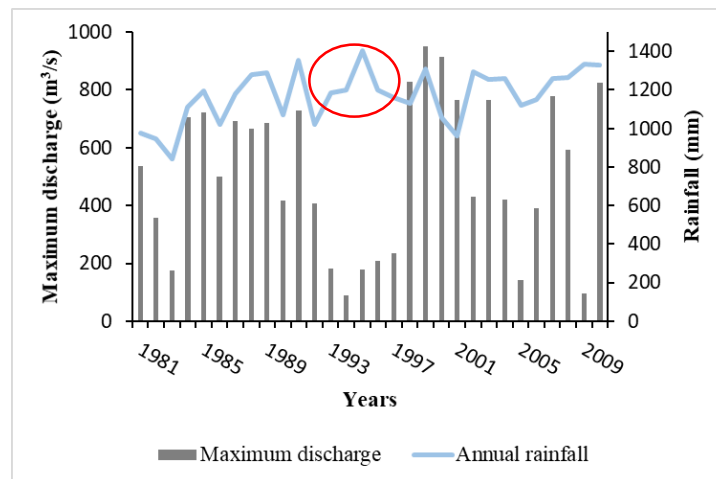


Figure 11: Trend of maximum discharge at Athiémé and annual rainfall in Mono watershed

On a visual inspection, the variations of maximum discharge match the one of annual rainfall — when rainfall decreases, discharge decreases as well —, except during the period 1993-1997 (circled with red on Figure 11) which may be due to missing values in discharge time series.

Furthermore, as depicted on Figure 12, the mean hydrograph over the period 1981-2010 reveals that discharge increases from June, peaks in September-October, then decreases. In addition, the minimum discharge value is 36.3 m³/s — greater than 0 —, and this means that Mono is a permanent river. However, it is worth noting that this mean hydrograph does hide periods in which the flow is very low (almost null).

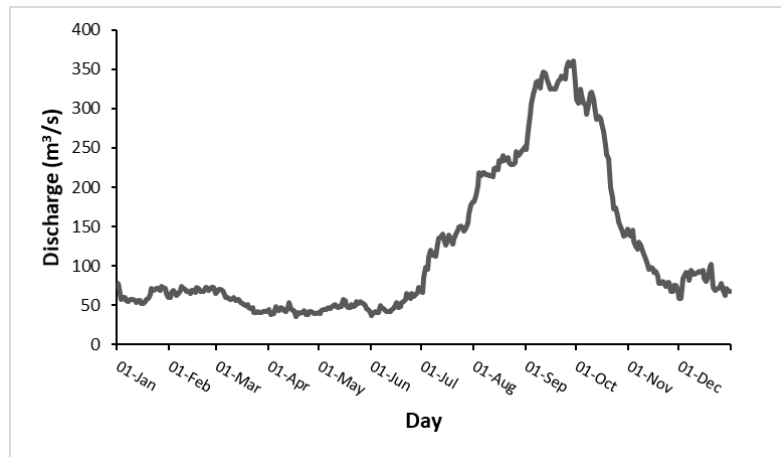


Figure 12: Mean hydrograph of Mono river during 1981-2010

4.1.2. Projected Climate

Before analysing projected climate in the watershed, observed climate variables (rainfall and precipitation) are compared to the corrected data simulated by the regional climate model REMO (Figure 13 and Figure 14).

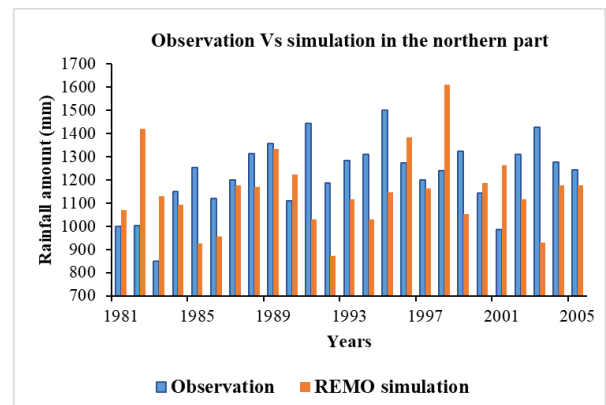
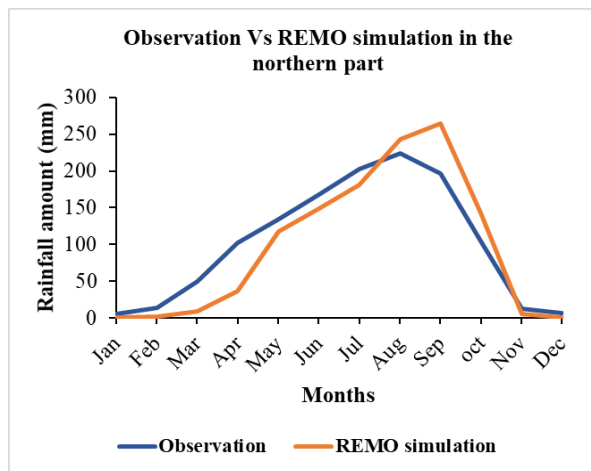
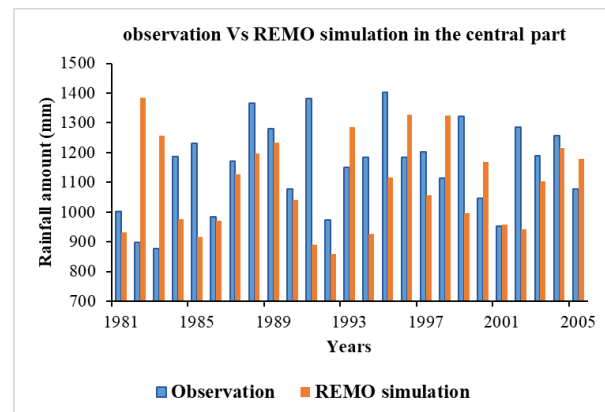
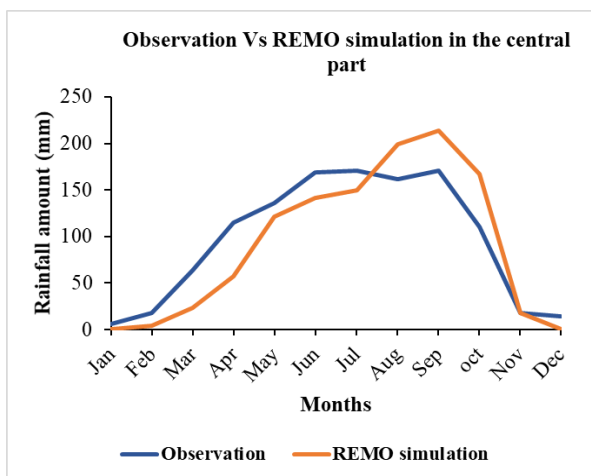
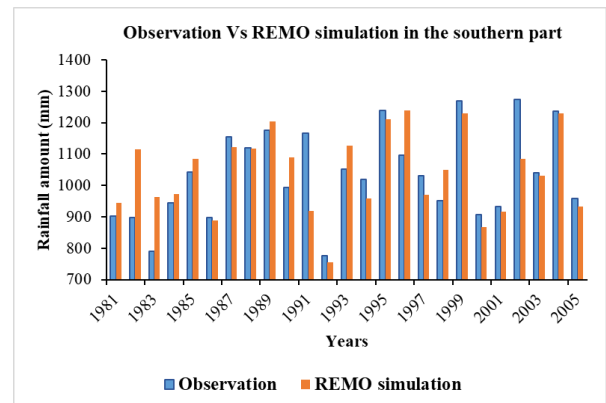
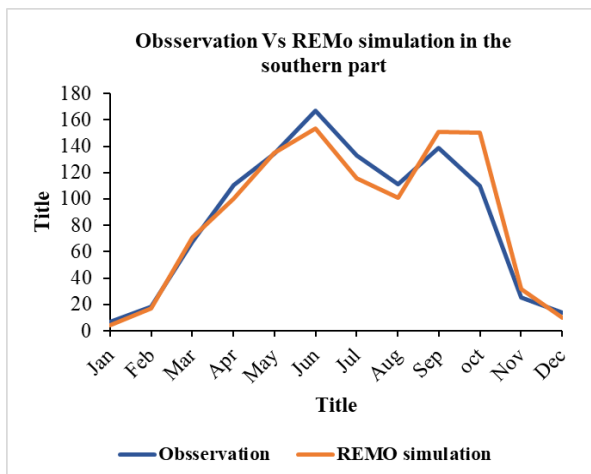


Figure 13: Comparison of observed and simulated rainfall, seasonal cycles (left) and annual rainfall (right)

The match seems better in the southern part in comparison with the central and northern parts where simulations show later onset of rainfall and higher peaks. However, rainfall offsets match.

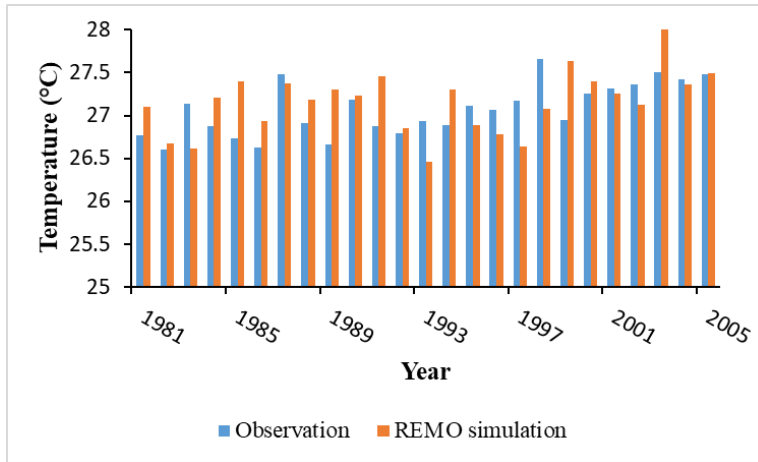


Figure 14: Comparison of observed and simulated temperature

It can be concluded that REMO simulates in an acceptable way temperature in Mono watershed. Globally after correction, biases in rainfall and temperature data are reduced compared to the raw outputs from REMO.

4.1.2.1. Projected Rainfall Patterns under RCP 4.5 and RCP 8.5

In the southern part, rainfall seasonal cycle will keep a bimodal pattern under RCP 4.5 and RCP 8.5. In addition, both scenarios project almost the same pattern. As in the normal period, the first peak is recorded in June but with a lower amount. However, the second peak which normally occurs in September will be extended to October with a higher value (see Figure 15).

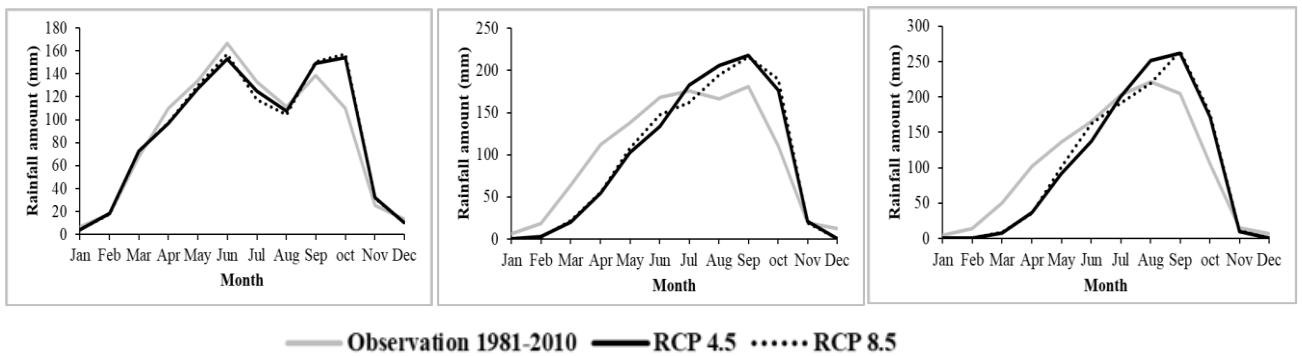


Figure 15: Seasonal cycles of the south (left), centre (middle) and north (right) parts under RCP 4.5 and RCP 8.5

In the central part, RCP 4.5 and RCP 8.5 project a unimodal regime characterized by (i) late onsets of rainfall; and (ii) lower precipitation from December to July for RCP 4.5, and august for RCP

8.5. In addition, both scenarios converge on the fact that the highest rainfall amount (about 217 mm) will be recorded in September.

In the north, rainfall will keep its unimodal pattern under both scenarios with (i) late onset of rainfall; and (ii) lower amounts from December to July for RCP 4.5 and august for RCP 8.5. The peak usually recorded in August (205 mm) will (i) shift to September; (ii) exceed and reach about 262 mm for RCP 4.5 and 265 mm for RCP 8.5.

Figure 16 depicts how the rainfall seasonal cycle is expected to change under RCP 4.5 and RCP 8.5, compared to the normal period.

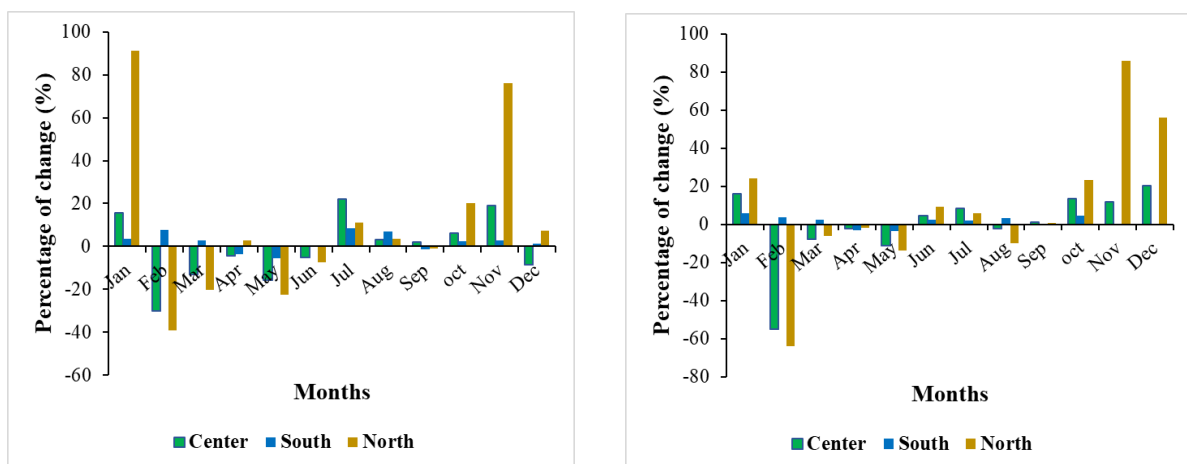


Figure 16: Expected change in seasonal cycles under RCP 4.5 (left) and RCP 8.5 (right)

Under RCP 4.5, the relative change in monthly rainfall varies from -5.5% to 8.4% in the southern part, -29.9% to 22.2% in the central part; and -39% to 91.4% in the northern part. And for RCP 8.5, the expected change ranges from -3.5% to 5.8% in the southern part, -55% to 20% in the central part and -64% to 85.9% in the northern part.

The results of Mann-Kendall test performed on annual rainfall under RCP 4.5 and RCP 8.5 are summarized in table 8. Those of homogeneity tests are in table 9.

Table 8: Results of Man-Kendall test on annual rainfall under RCP 4.5 and RCP 8.5

Scenario	Region	tau	p.value	Conclusion
RCP 4.5	South	-0.0152	0.9136	<i>Decreasing but not significant trend</i>
	Centre	0.1326	0.2850	<i>Increasing but not significant trend</i>
	North	0.2083	0.0912	<i>Increasing but not significant trend</i>
RCP 8.5	South	-0.0682	0.5876	<i>Decreasing but not significant trend</i>
	Centre	-0.0568	0.6531	<i>Decreasing but not significant trend</i>
	North	0.1061	0.3941	<i>Increasing but not significant trend</i>

Table 9: Results of homogeneity tests on annual rainfall under RCP 4.5 and RCP 8.5

Scenario	Region	Result	Breakpoint	p.value	Conclusion
RCP4.5	South	Pettitt's test	2021	1.6211	<i>There is no change in rainfall time series</i>
		SNH test	2049	0.9429	
	Centre	Pettitt's test	2033	0.3466	
		SNH test	2033	0.5255	
	North	Pettitt's test	2031	0.1293	
		SNH test	2031	0.1547	
RCP 8.5	South	Pettitt's test	2029	1.0728	<i>There is no change in rainfall time series</i>
		SNH test	2024	0.8421	
	Centre	Pettitt's test	2029	0.6727	
		SNH test	2029	0.7116	
	North	Pettitt's test	2041	0.3238	
		SNH test	2041	0.1044	

The results of homogeneity tests and Mann-Kendall test suggest that all over the watershed, there is neither breakpoint nor linear trend in annual rainfall time series, under emission scenarios RCP 4.5 and RCP 8.5. Statistical wise, rainfall time series are homogenous and present no trend. Nonetheless, as depicted by Figure 17 and Figure 18, some variabilities are observed.

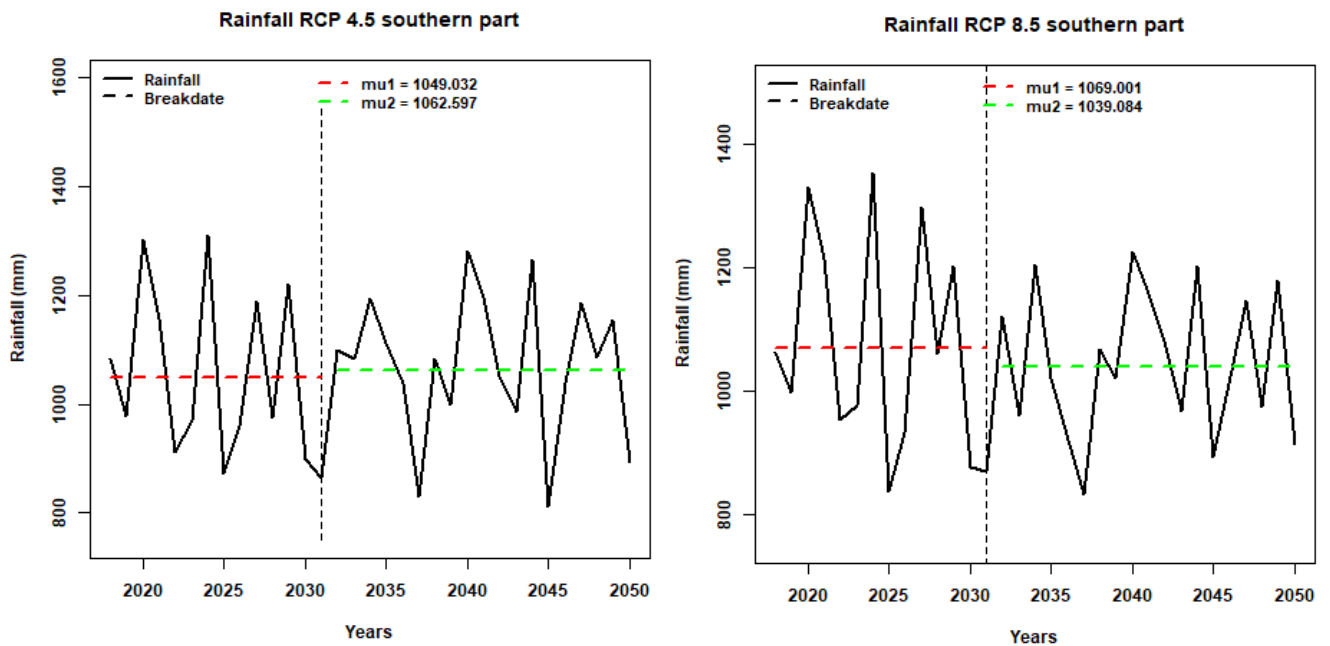


Figure 17: Pattern of annual rainfall in the southern part under RCP 4.5 and RCP 8.5

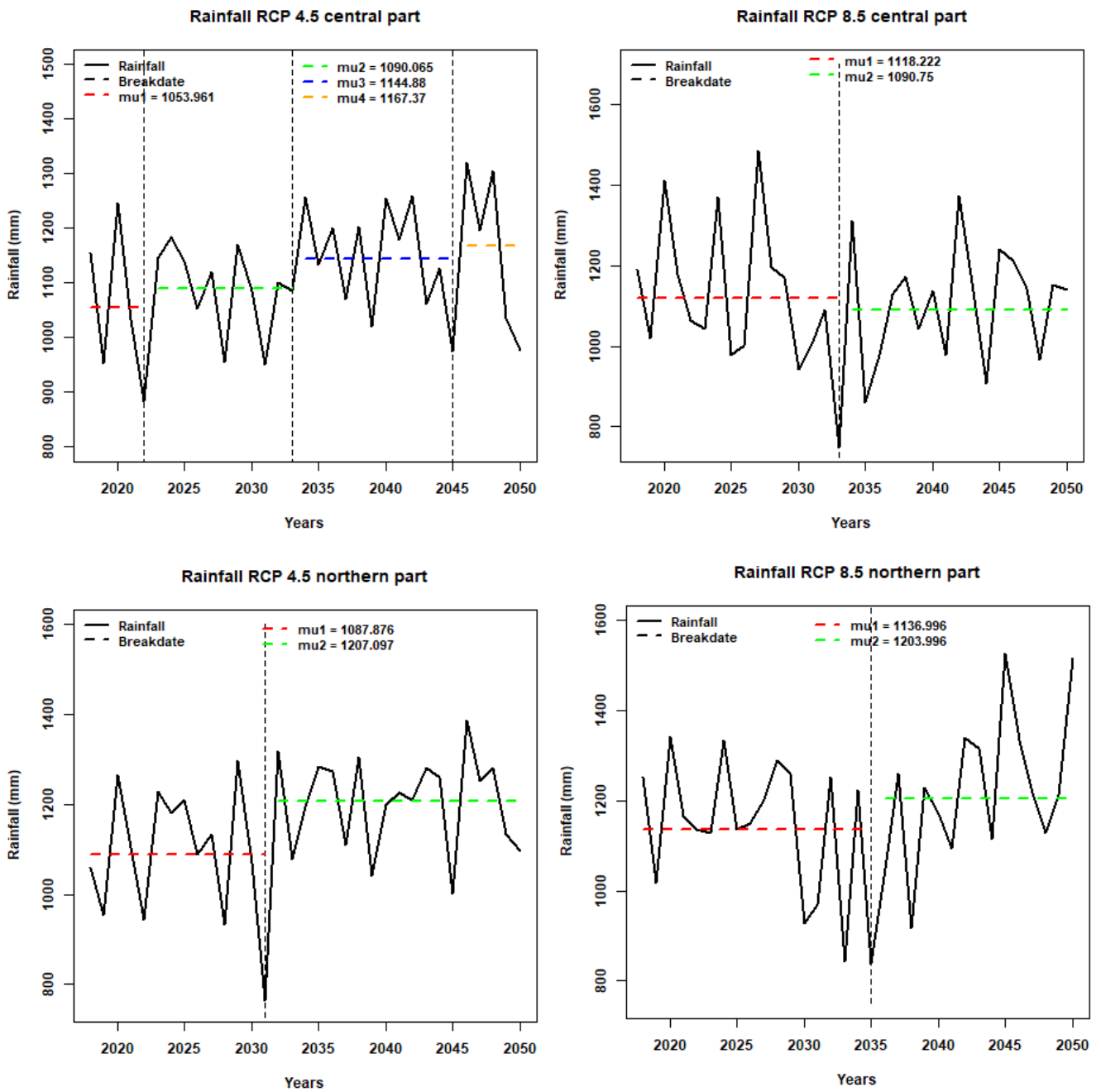


Figure 18: Pattern of annual rainfall in the central and northern part under RCP 4.5 (left) and RCP 8.5 (right)

Figure 19 presents the standardized precipitation indexes (SPI) computed under RCP 4.5 and RCP 8.5

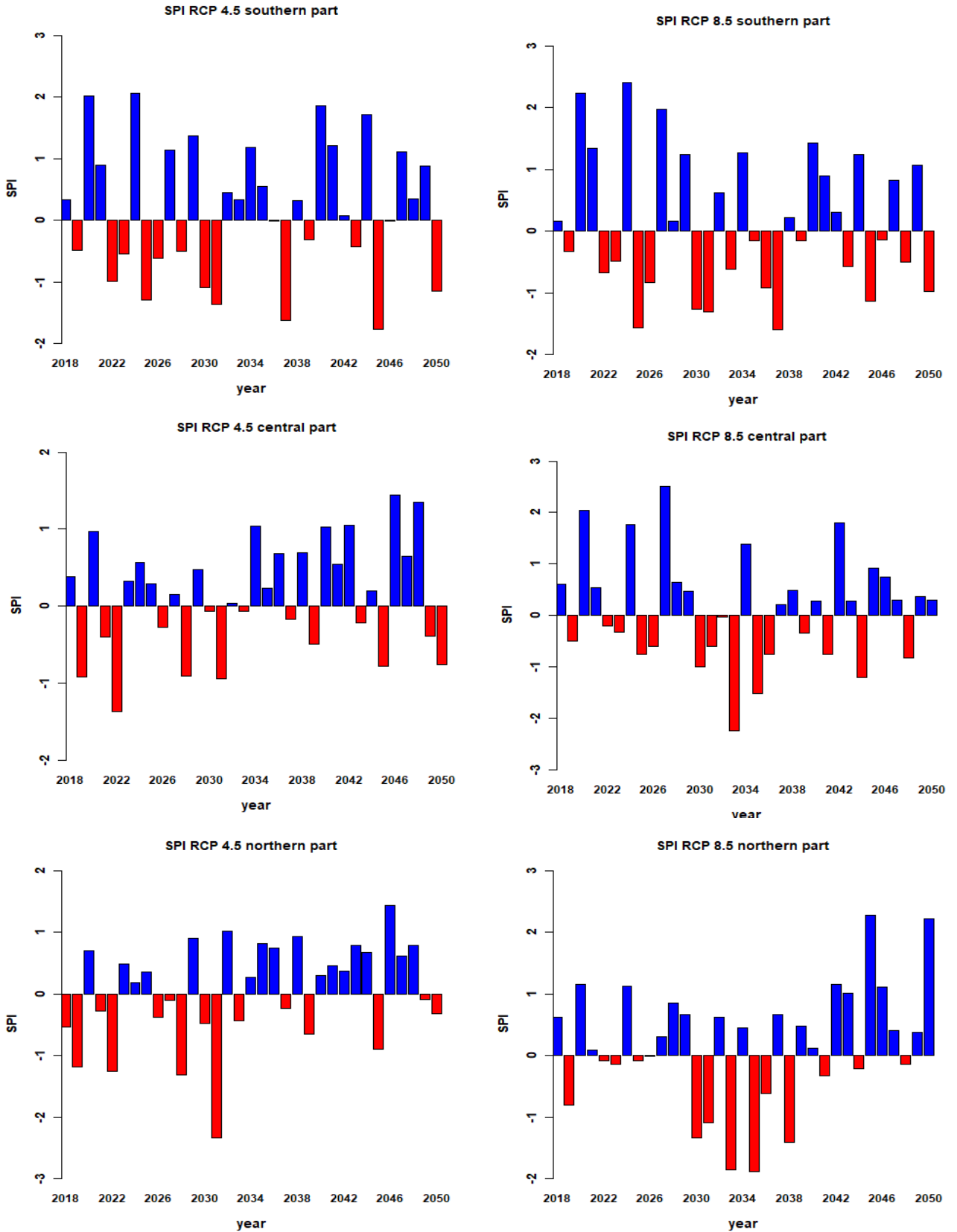


Figure 19: Standardized Precipitation Index of annual rainfall in southern, central and northern part under RCP 4.5 (left) and RCP 8.5 (right)

Using RCP 4.5, the number of deficit year in the watershed increases upward, 13 years in the south, 14 in the centre and 15 in the north. The years 2020 and 2024 will be extremely wet in the south whereas 2031 will be extremely dry in the north. On the other side, the number of deficit years decreases upward for RCP 8.5, 17 years in the south, 14 in the central part and 13 in the north. 2033 will be extremely dry in the north, and again, years 2020 and 2024 for this scenario will be extremely wet in the south. One can notice that from south to north, RCP 8.5 projects more extremely wet years — 6 — than RCP 4.5 does — 2.

4.1.2.2. Projected Temperature Patterns under RCP 4.5 and RCP 8.5

Under RCP 4.5, the homogeneity tests detected breakpoints at different dates –SNH 2027; Pettitt 2031— but they got an agreement under RCP 8.5 –2038 (Figure 20).

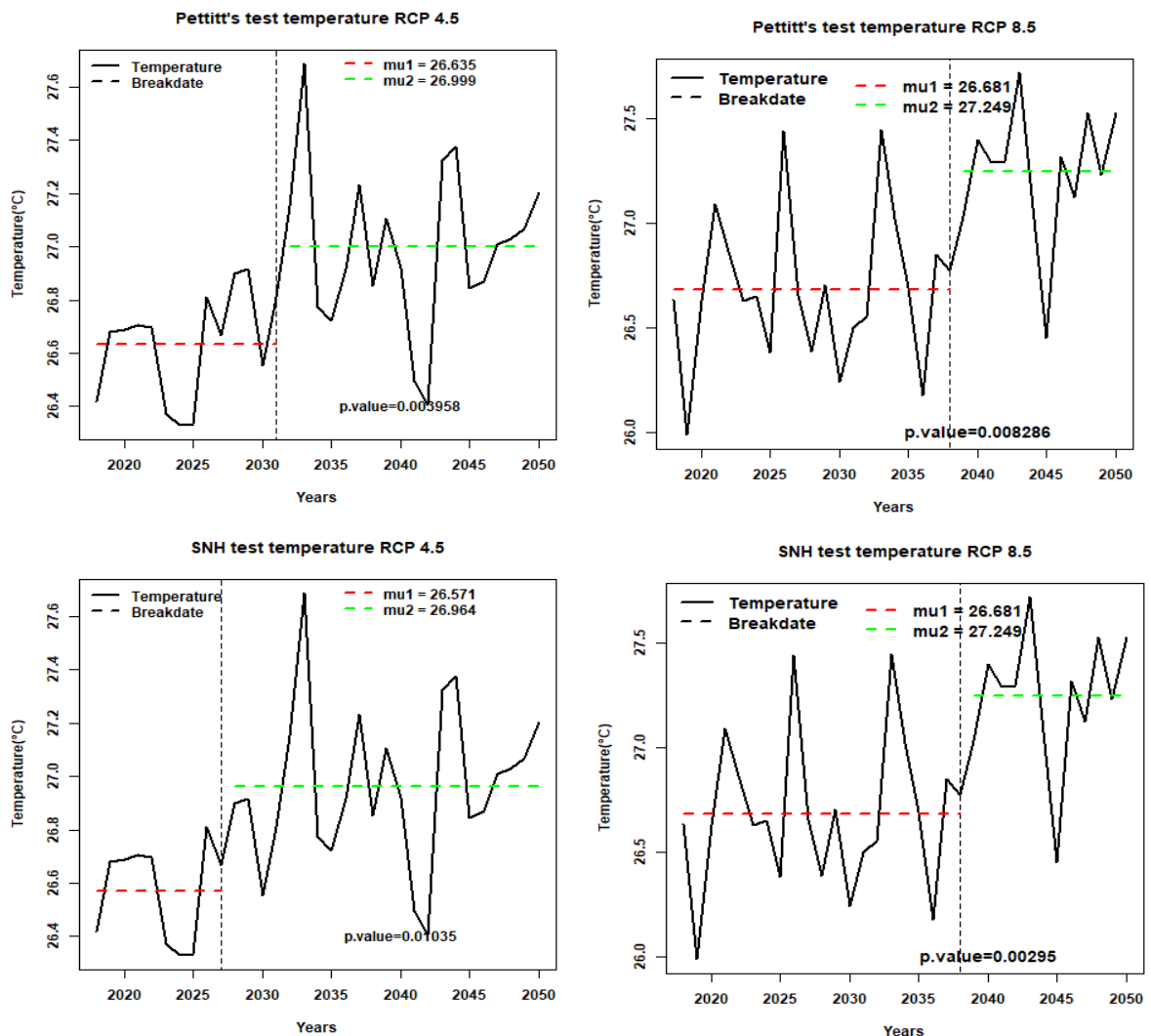


Figure 20: Homogeneity tests performed on temperature under RCP 4.5 and RCP 8.5

In addition, both scenarios project an increasing and significant trend for temperature by 2050 (Table 10). This results corroborates projected trends at global scale and regional scale.

Table 10: Results of Man-Kendall test on annual temperature under RCP 4.5 and RCP 8.5

Scenario	tau	p.value	Conclusion
RCP 4.5	0.4	0.0003	<i>Increasing and significant trend</i>
RCP 8.5	0.4	0.0009	<i>Increasing and significant trend</i>

Figure 21 depicts anomalies of temperature under RCP 4.5 and RCP 8.5

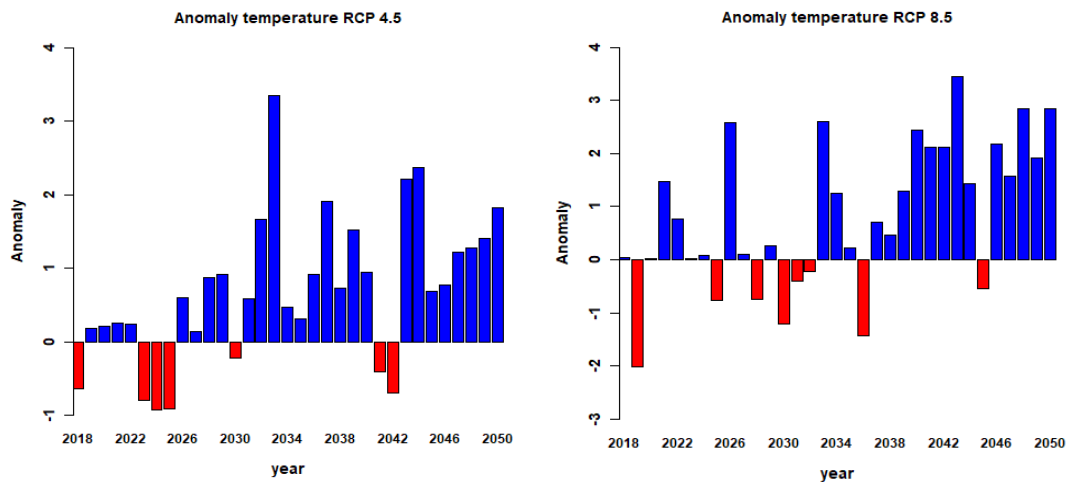


Figure 21: Temperature anomaly under RCP 4.5 and RCP 8.5

There are 26 years above normal under RCP 4.5, whereas 25 are recorded for RCP 8.5. As for years below normal, they are 7 under the former scenario and 8 under the latter. Future climate will be warmer.

4.2. Discharge simulation

4.2.1. Sensitivity analysis

On assessing the sensitivity of each parameter, it was noticed that R^2 was greater than 0.5 for parameters K1 (storage or recession coefficient), FC (maximum soil moisture storage), LP (soil moisture value above which AET reaches PET), and BETA (determines the relative contribution

to runoff from rain or snowmelt), meaning that they are the ones NSE depends most on. However, LP happens to be the most sensitive to variations.

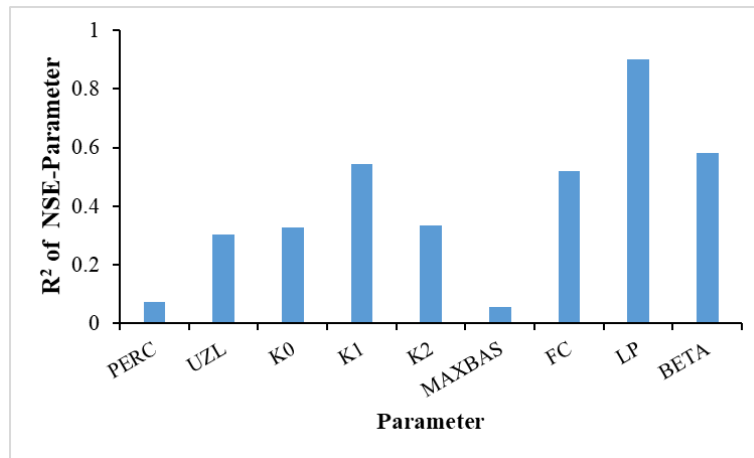


Figure 22: Sensitivity analysis of the parameters of HBV-light

4.2.2. Calibration and validation

As presented by Figure 23 there is a good match between observed and simulated discharge in calibration period, but less satisfactory in validation where peaks seem not to be well modelled.

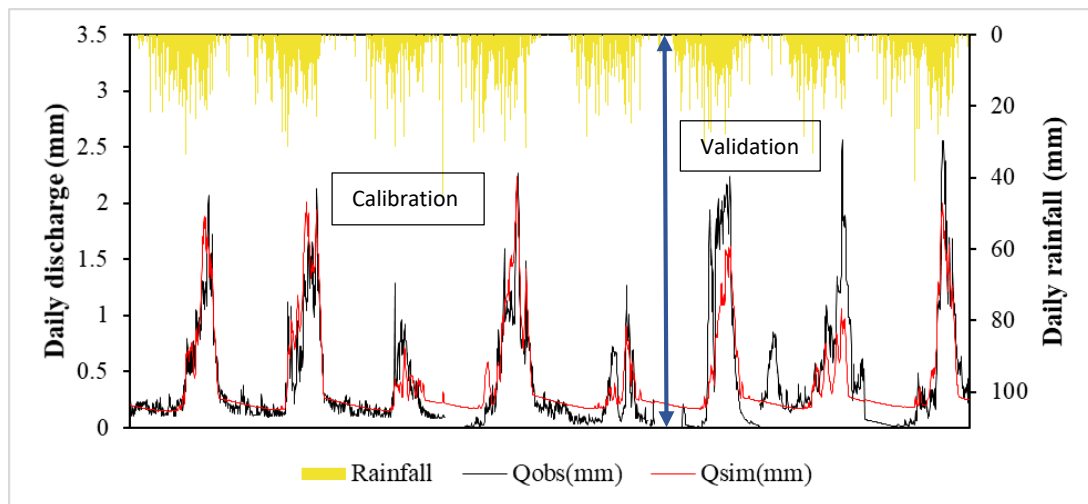


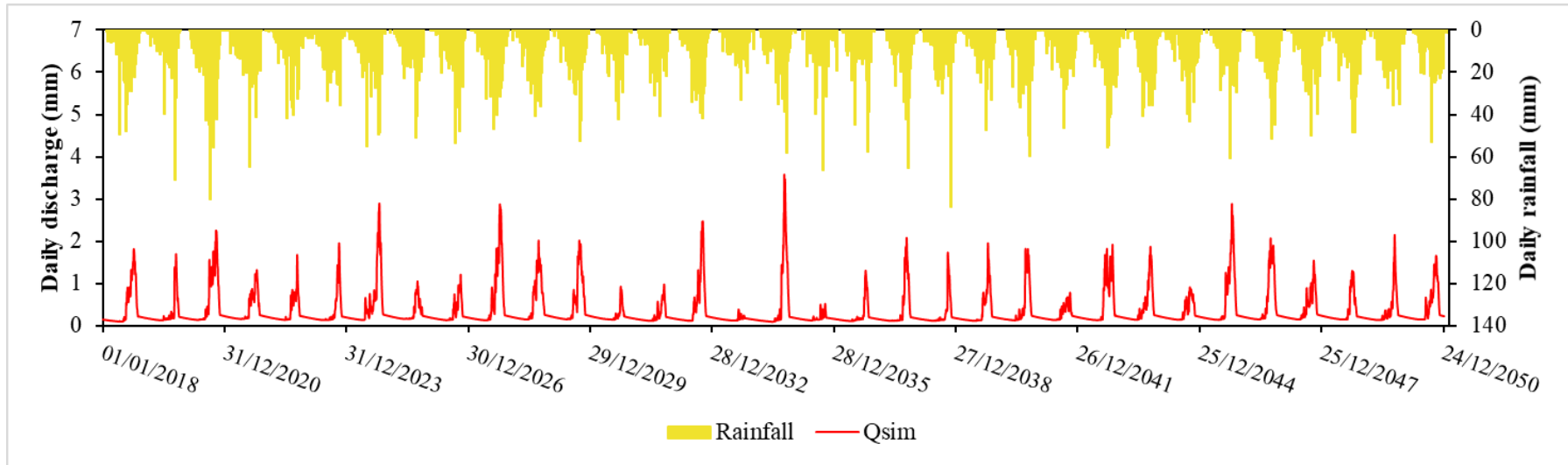
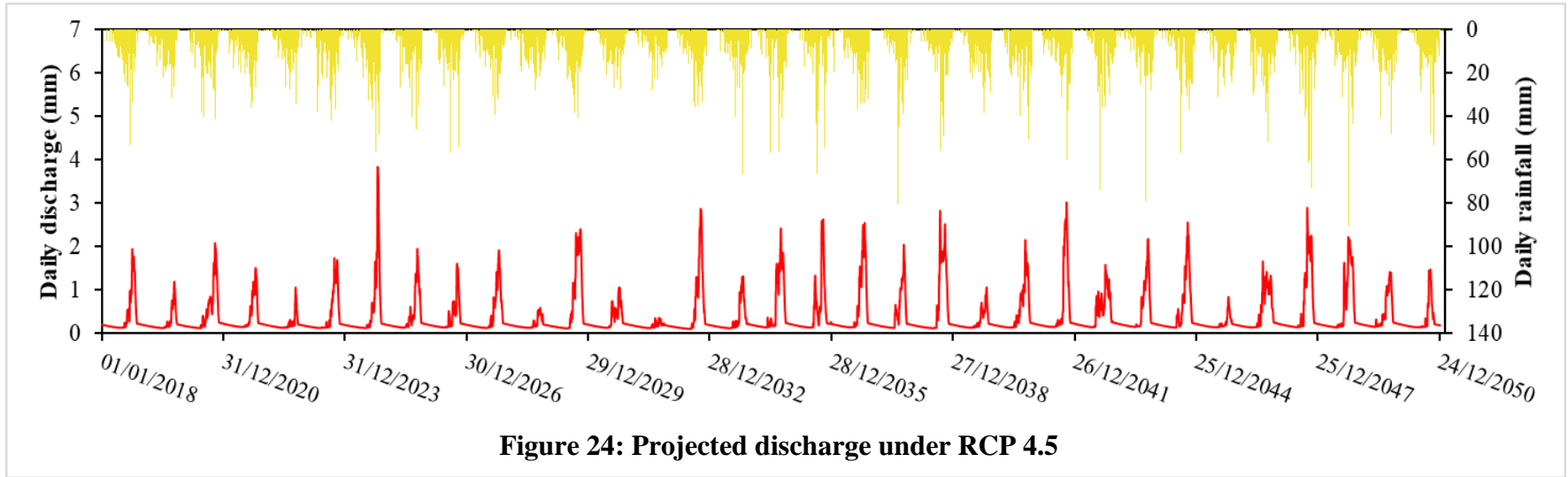
Figure 23: Calibration and validation of HBV-light

The objective function, Nash-Sutcliff Efficiency coefficient (NSE) delivered good values, 0.79 during calibration and 0.67 in validation. The percent of bias (PBIAS) equals 16.1% in calibration, indicating an overestimation, and -14.4% in validation, indicating underestimation. R² reached 0.83 and 0.73 respectively in calibration and validation. Globally, the ranges of these criteria

implies that HBV-light provides good results for discharge simulation in Mono watershed – Athiémé.

4.2.4. Expected discharges under RCP 4.5 and RCP 8.5

The future discharge as simulated by HBV-light is presented on Figure 24 and Figure 25 respectively for scenario RCP 4.5 and RCP 8.5. The projected discharges present high inter-annual variability. The results of Mann-Kendall test over the period 2018-2050 revealed an increasing but not significant trend for RCP 4.5 ($\tau = 0.106$; pvalue = 0.394), whereas a decreasing but not significant trend was detected for RCP 8.5 ($\tau = -0.036$; pvalue = 0.78). Under the first scenario, maximum discharge ranges from 116 m³/s to 1236 m³/s, with the lowest value in 2031 and the highest in 2024. As for RCP 8.5, it projects Mono River discharge at Athiémé to vary between 123 m³/s and 1150 m³/s with the lowest value in 2033 and the highest being in 2034.



Moreover, the mean hydrograph is expected to change in the next 33 years compared to the period 1981-2010 (Figure 26). Under RCP 4.5 and RCP 8.5, the period of low water will last from December to July, unlike during 1981-2010 where it was from July to November. In addition, the high flow period will shorten and the peak will then occur in October. Globally, the mean hydrograph will shift rightward, increase in amplitude and high flow period will shorten. Indeed the rational of such changes can be found in the fact that rainfall in central and northern parts are expected to (i) have later onset, (ii) last shorter and, (iii) have higher peaks. This corroborates the findings of Amoussou (2010) that high water flow at Athiémé is linked to maximum rainfall in the tropical regions of the watershed (centre and north).

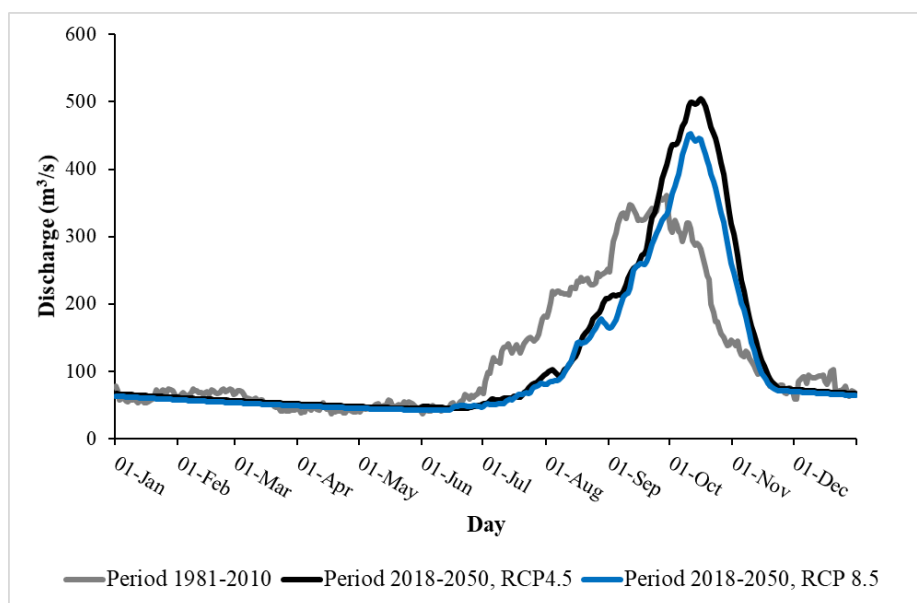


Figure 26: Mean hydrograph at Athiémé for the normal period and the period 2018-2050 under RCP 4.5 and RCP 8.5

4.3. Implication of Projected Discharges for Infrastructures and Human Security

4.3.1. Existing Threats/Background

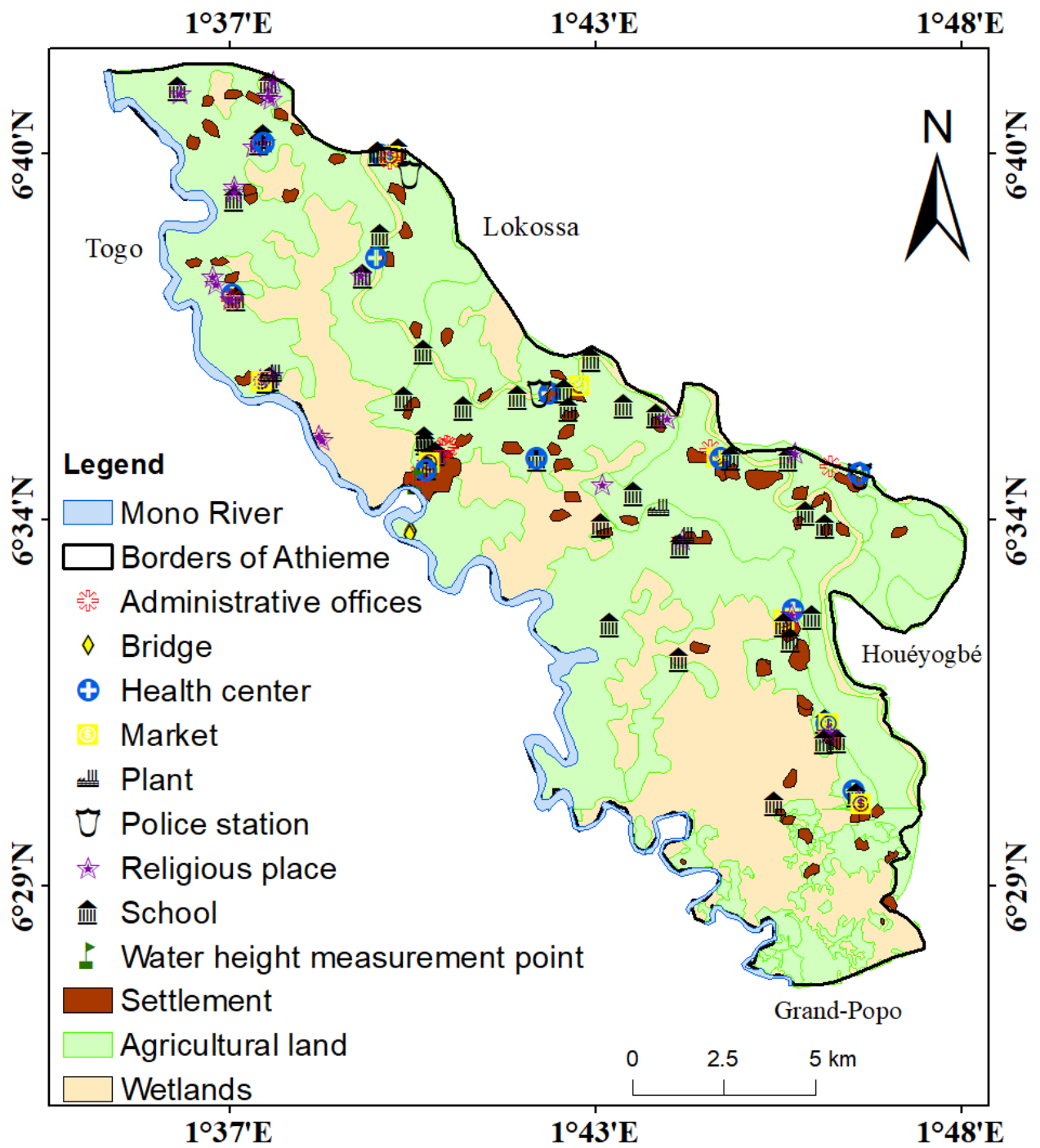
Land Use/land cover has substantially changed in the watershed during the last three decades (Table 11; Annex 1; Annex 2).

Table 11: Evolution of land use/land cover in Mono watershed

Features of land use/land cover	Area surface (ha)		percentage of change (%)	Comment
	1980	2015		
Gallery Forest	91627	74542	-18.64625056	<i>Regression</i>
Dense Forest	434504	36994	-91.48592418	<i>Regression</i>
Woodlands	813353	331248	-59.27377166	<i>Regression</i>
Wooded savannah	692301	459814	-33.58178018	<i>Regression</i>
Savannah	22883	22883	0	<i>Stability</i>
Cropland and fallow with palm trees	309329	120189	-61.14525311	<i>Regression</i>
Mangrove	40369	12021	-70.2222002	<i>Regression</i>
Wetlands	43373	26168	-39.6675351	<i>Regression</i>
Fourré	153050	22427	-85.34661875	<i>Regression</i>
Cropland and fallow	48203	1221279	2433.616165	<i>Increase</i>
Plantation	5223	323049	6085.123492	<i>Increase</i>
Water bodies	48503	48503	0	<i>Stability</i>
Settlements	79550	83151	4.526712759	<i>Increase</i>
Total	2782268	2782268		

In fact, land use by human has increased to the detriment of natural land cover. Forest lands and mangroves decreased whereas, settlements and agriculture lands have increased. Dwindling of forests wetlands, and mangrove represents a threat for people in Mono watershed, because it will favour more surface runoff and lower infiltration. Especially, communities like Athiémé which are located downstream might experience the severer consequences.

Figure 27 presents infrastructures and agricultural lands in Athiémé. The features displayed on that map are determinant for human security, namely for: economic, environmental, social, political, personal, health and food security. As shown on the map, infrastructures are stuck up and this may increase the array of loss in case of hydrological disasters.



Source: CENATEL; Field work: 2017

Figure 27: Land use and land cover map of Athiémé

4.3.2. Projected Impacts

Figure 28 compares maximum discharge during the period 2018-2050 with those of years 1983 (reference for low discharge) and 2010 (reference for high discharge).

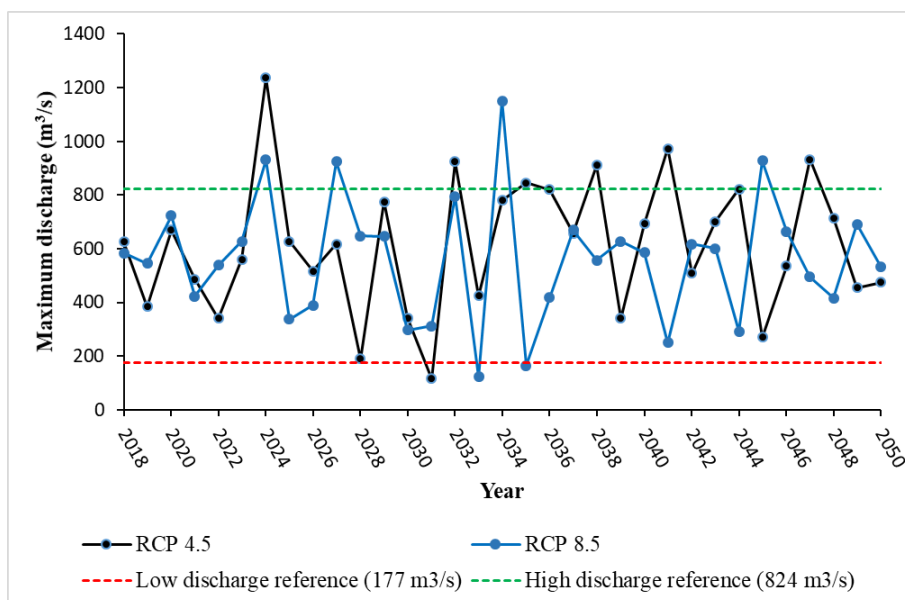


Figure 28: Projected maximum discharge under RCP 4.5 and RCP 8.5

It is worth noting that both high and low flow are expected in two contiguous years under RCP 4.5 — 2031, 2032 — and three under RCP 8.5 (2033, 2034, 2035). This means that Athiémé will likely experience consecutive disastrous events in these periods. Then preparedness and adaptation strategies need to be developed accordingly.

The potential impacts of Mono river flow on the communities of Athiémé are first of all presented for the scenario RCP 4.5 and afterwards for RCP 8.5.

4.3.2.1. Scenario RCP 4.5

This scenario projects substantial drought related impacts for years 2028, 2031, whereas years 2024, 2032, 2035, 2036, 2038, 2040, 2044, 2047 will likely bring about substantial damages relating to flood. Figure 30 presents chronological maps of flood prone areas in Athiémé, from 2020 to 2050. A time step of 5 years is considered (2020, 2025, 2030, 2035, 2040, 2045 and 2050) in addition to years 2024 and 2031 corresponds to highest and lowest discharge for RCP 4.5.

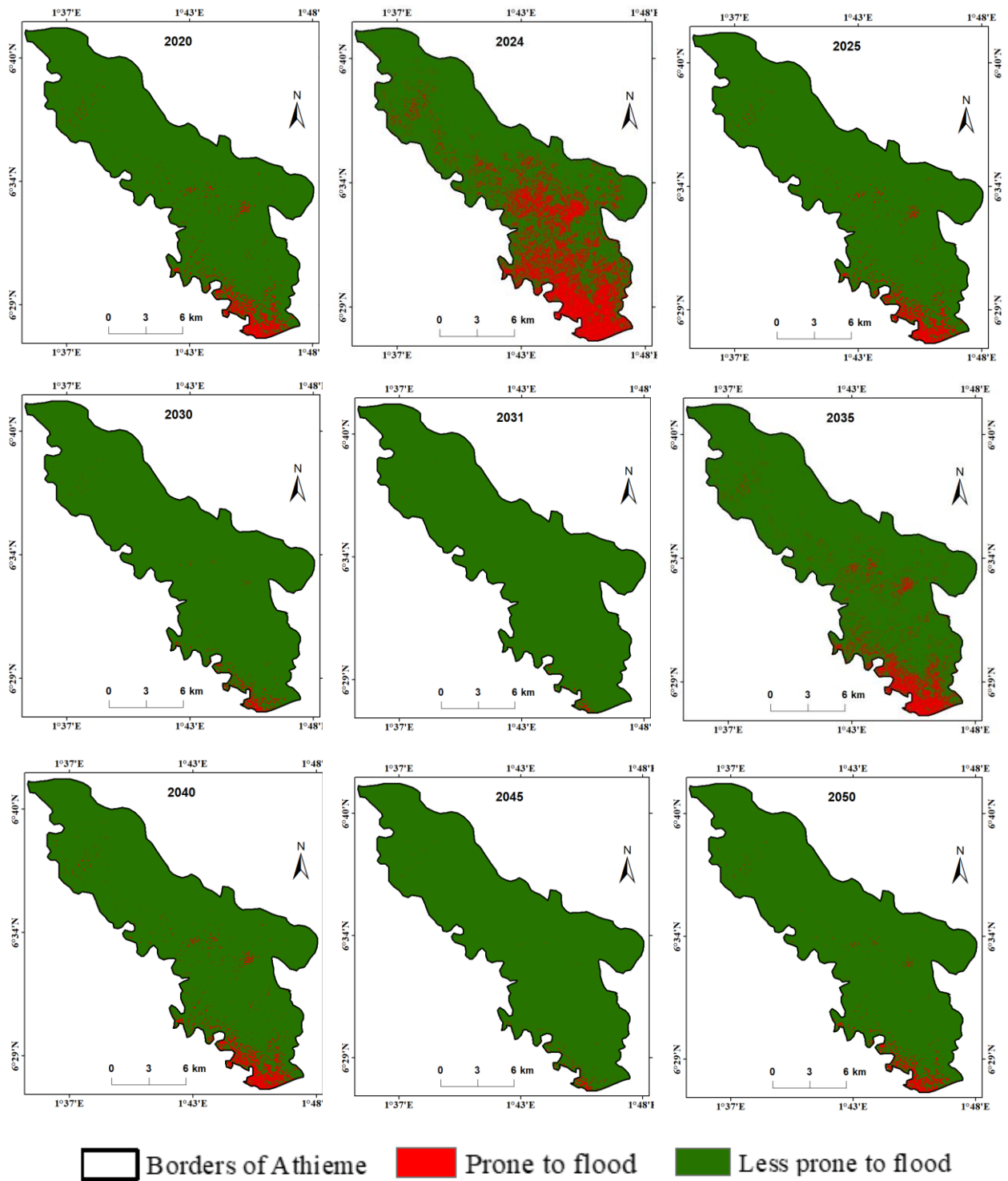


Figure 29: Flood prone areas in Athiémé from 2020 to 2050

The land surface corresponding to areas threatened by flood are presented in Table 12.

Table 12: Proportion of flood prone areas under RCP 4.5

Year	Threatened area %	Affected districts (flood spot)
2020	14.44	Athiémé, Atchannou, Adohoun, Kpinnou, Dédékpòè
2024	20.11	Athiémé, Atchannou, Adohoun, Kpinnou, Dédékpòè
2025	14.05	Athiémé, Atchannou, Adohoun, Kpinnou, Dédékpòè
2030	10.33	Athiémé, Atchannou, Kpinnou, Dédékpòè
2031	6.26	Athiémé, Atchannou, Dédékpòè
2035	16.43	Athiémé, Atchannou, Adohoun, Kpinnou, Dédékpòè
2040	14.80	Athiémé, Atchannou, Adohoun, Kpinnou, Dédékpòè
2045	9.22	Atchannou, Atchannou, Dédékpòè
2050	12.91	Athiémé, Atchannou, Adohoun, Kpinnou, Dédékpòè

4.3.2.2 Scenario RCP 8.5

Under this scenario, it is likely that in years 2033 and 2035 Athiémé will experience drought and with comparable damage as in 1983. On the other side, disastrous flood events are expected in years 2024, 2027, 2032, 2034 and 2045 with reference to 2010's flood. As earlier done for the other RCP 4.5, maps of flood prone areas are presented (Figure 30) in a chronological way — 5 years time step — in addition to years 2033 (lowest flow) and 2034 (highest flow).

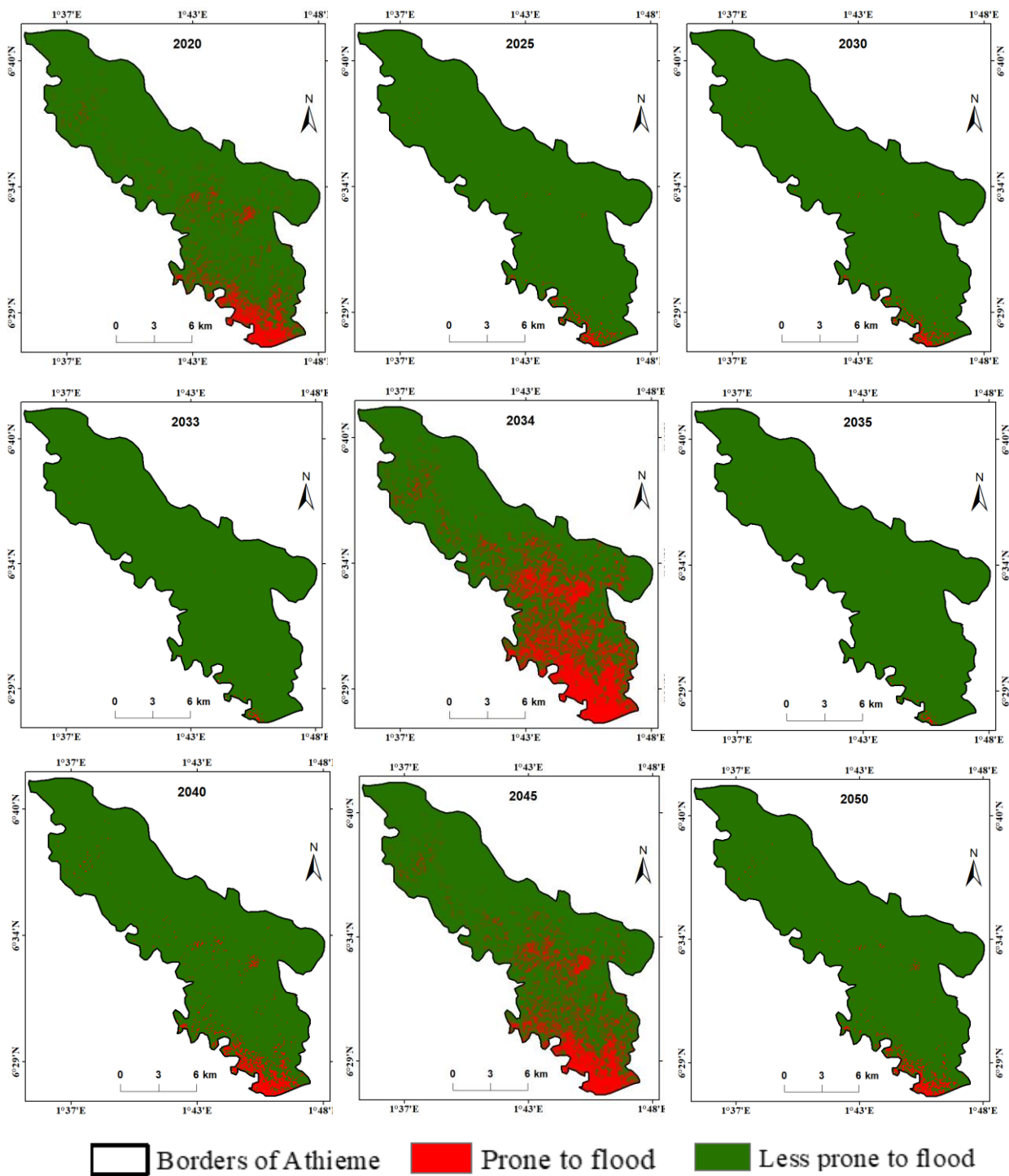


Figure 30: Flood prone areas in Athiémé from 2020 to 2050

The land surface corresponding to areas threatened by flood are presented in Table 13.

Table 13: Proportion of flood prone areas under RCP 8.5

Year	Threatened area %	Affected districts (flood spot)
2020	15.13	Athiémé, Atchannou, Adohoun, Kpinnou, Dédékpòè
2025	10.26	Athiémé, Atchannou, Kpinnou, Dédékpòè
2030	9.65	Athiémé, Atchannou, Kpinnou, Dédékpòè
2033	6.41	Atchannou, Dédékpòè
2034	19.26	Athiémé, Atchannou, Adohoun, Kpinnou, Dédékpòè
2035	7.31	Atchannou, Dédékpòè
2040	13.56	Athiémé, Atchannou, Adohoun, Kpinnou, Dédékpòè
2045	17.24	Athiémé, Atchannou, Adohoun, Kpinnou, Dédékpòè
2050	12.91	Athiémé, Atchannou, Adohoun, Kpinnou, Dédékpòè

4.3.2.3. General Comment

- Both scenarios RCP 4.5 and RCP 8.5, projected high discharge in years 2024, 2032 and 2034. This increases the likelihood of the projected impacts in those years.
- Even for years of lowest peak flow — lower than 200 m³/s, and lower than discharge value of 1983 —, there are still some places which are susceptible to be flooded. Those places are of very low elevation and located in flood plain. The projections showed that, among the 5 districts of Athiémé, Atchannou is every year the most affected — in terms of flooded area surface. This district needs then an appropriate flood management plan.
- Years of relatively low maximum flow do not bear the spectrum of disastrous flood, but might hide drought of water scarcity situations.

CHAPTER V: CONCLUSION AND POLICY RECOMMENDATIONS

The objective of this study was to assess the impact of climate change on Mono River downstream inflows by 2050. It was carried out using the regional climate model REMO, under the scenarios RCP 4.5 and RCP 8.5, the hydrological model HBV-light and digital elevation models (DEM) from the Shuttle Radar Topography Mission (SRTM).

The study discovered that, during the normal period 1981-2010, both temperature and rainfall have been increasing in the Mono watershed. For the period 2018-2050, rainfall in the southern Mono will (i) reduce slightly during the first rainy season and, (ii) increase during the second rainy season which will extend to October. In the central part, rainfall regime will henceforward be unimodal with late onset of rainfall and higher peaks (about 217 mm) recorded in September. Similarly, rainfall season in the north will start tardily and the peak will shift from August to September. In addition, annual rainfall in the future (2018-2050) will be characterised by high variability all over the watershed. As for temperature, it is expected to increase, under the two climate scenarios RCP 4.5 and RCP 8.5.

Given these new characteristics of the climate, the discharge of Mono river at Athiémé will undergo some modifications. Regardless of the scenario used, the hydrograph is expected to shift rightward, with a longer low flow period and increase of maximum flows. Moreover, under RCP 4.5, lowest and highest maximum flow will respectively be recorded in 2024 and 2031. However, drought events (like or severer than the one of 1983) are expected in 2028 and 2031; whereas in years 2024, 2032, 2035, 2036, 2038, 2040, 2044, 2047 substantial damages relating to floods (as or higher than those of 2010) are likely to take place. Flood prone areas range from 6.26% to 20.11% of Athiémé's land surface. On the other side, the scenario RCP 8.5 projects highest and lowest maximum flow to occur respectively in 2034 and 2033. In addition, it is likely that Athiémé will experience drought in years 2033 and 2035 (with associated damages comparable or higher than those of 1983); but disastrous flood events are rather expected in years 2024, 2027, 2032, 2034 and 2045 with reference to 2010's flood. As a result, between 6.41% and 19.26% of Athiémé's land surface will be flooded. Furthermore, the district of Atchannou will probably be the most affected by the projected flood events.

It is thus important to pursue and strengthen existing flood management strategies in Athiémé. For instance, a thorough flood risk assessment is required in order to undertake relevant actions. Even if Athiémé experiences more flood events than drought, the occurrence of the latter should not be underestimated, considering the high variability projected in the climate of Mono watershed. Furthermore, adaptation and contingency plans should not focus only on Athiémé, but rather involve all the communities located in Mono watershed, either upstream or downstream.

Moreover, this study paves way for further scientific researches:

- Use more than one climate model (ensemble modelling),
- Assess other climate trend analysis methods,
- Assess the capability of other hydrological models at simulating discharge in Mono watershed,
- Use hydrological models which account for land use.

References

1. Ago, E.E., F. Petit, and P. Ozer. 2005. Analyse des Inondations en Aval du Barrage de Nangbeto sur le Fleuve Mono (Togo et Bénin). *Geo-Eco-Trop* 29: 1–14.
2. Amoussou, E. 2010. *Variabilité Pluviométrique et Dynamique Hydro-Sédimentaire du Bassin Versant du Complexe Fluvio-lagunaire Mono-Ahémé-Couffo (Afrique de l'ouest)*, Phd dissertation : Universite de Bourgogne, France.
3. Amoussou, E., P. Camberlin, S. H. Totin Vodounon, Trambly, P., C. Houndenou, G. Mahé, J-E. Paturel. 2014. Evolution des précipitations extrêmes dans le bassin versant du Mono (Bénin-Togo) en contexte de variabilité/changement climatique. *XXVIIe Colloque de l'Association Internationale de Climatologie, Dijon 2014*, 331-337.
4. Amoussou, E. 2015. Analyse Hydrométéorologique des Crues dans le Bassin-versant du Mono en Afrique de l'Ouest avec un Modèle Conceptuel Pluie-Débit. *FMSH-WP 90*: 27pp.
5. Amoussou, E., S.H. Totin Vodounon, S. Houessou, Y. Trambly, P. Camberlin, C. Houndenou, M. Boko, G. Mahe, and J-E. Paturel. 2015. Application d'un Modèle Conceptuel à l'Analyse de la Dynamique Hydrométéorologique des Crues dans un Bassin-versant en Milieu Tropical Humide : Cas du Fleuve Mono. *XXVIIIe Colloque de l'Association Internationale de Climatologie, Liège 2015*, 17–24.
6. Babur, M., M. S. Babel, S. Shrestha, A. Kawasaki, and N. K. Tripathi. 2016. Assessment of Climate Change Impact on Reservoir Inflows Using Multi Climate-Models under RCP's—the Case of Mangla Dam in Paskitan. *Water* 8(389): 28pp.
7. Badjana, H. M. 2015. River basins assessment and hydrologic processes modeling for Integrated Land and Water Resources management (ILWRM) in West Africa. Phd dissertation, Université d'Abomey-Calavi.
8. Badou, F.D. 2016. Multi-Model Evaluation of Blue and Green Water Availability under Climate Change in four-non Sahelian Basins of the Niger River Basin. PhD dissertation, Université d'Abomey-Calavi.
9. Baillargeon, S. 2005. Le krigeage : *Revue de la théorie et application à l'interpolation spatiale de données de précipitations*. Master's thesis, Université Laval.
10. Bates, B. C., Z. W. Kundzewicz, S. Wu, and J. Palutikof. 2008. *Climate Change and Water. Technical Paper of the Intergovernmental Panel on Climate Change*. Geneva, IPCC Secretariat.

11. Biao, E.I. 2017. Assessing the impacts of climate change on river discharge dynamics in Ouémé river basin (Benin, West Africa). *Hydrology* 4(47):2-16
12. Bontogho, T-N. P. E. 2015. *Modeling a sahelian water resource allocation under climate change and human pressure: case of Loumbila dam in Burkina Faso*.
13. Christensen, J.H., F. Boberg, O. B. Christensen, and P. Lucas-Picher. 2008. On the need for bias correction of regional climate change projections of temperature and precipitation. *Geophys. Res. Lett.* 35 (20).
14. Collins, J. M. 2011. Temperature variability over Africa. *Journal of climate*. (24): 3649-3665.
15. Driessen, T. L. A., R. T. W. L. Hurkmans, W. Terink, P. Hazenberg, P. J. J. F. Torfs, and R. Uijlenhoet. 2010. The hydrological Response of the Ourthe Catchment to Climate Change as Modelled by the HBV Model. *Hydrology and Earth System Sciences*. 14(2010): 651–665.
16. Duaibe, K. 2008. *Human Activities and Flood Hazards and Risks in the South West Pacific: a case study of the Navua Catchment Area, Fiji Islands*, Masters thesis: Victoria University of Wellington.
17. EM-DAT: The OFDA/CRED International Disaster Database, Université catholique de Louvain: Brussels, Belgium. <http://www.emdat.be/>. Accessed on 17/04/2017.
18. Essou, G. RC. ; and F. Brissette. 2013. Climate change impacts on the Ouémé River, Benin, West Africa. *Earth Science and Climatic Change*. 4(6): 1-10.
19. Fang, G., Yang, J., Chen, Y. N. and Zammit, C, Comparing bias correction methods in downscaling meteorological variables for a hydrologic impact study in an arid area in China. 2015. *Hydrology and Earth System Sciences*. 2015: 2547–2559
20. Gaba, O. U. C., I. E. Biao, A. E. Alamou, and A. Afouda. 2015. An Ensemble Approach Modelling to Assess Water Resources in the Mékrou Basin, Benin. *Science Publishing Group* 3(2): 22–32.
21. Gayathri, K.D., B. P. Ganasri, G. S. Dwarakish. 2015. A review on hydrological models. *Aquatic Procedia*. 4(2015): 1001-1007.
22. Gupta, H. V., S. Sorooshian, and P. O. Yapo, 1999. Status of automatic calibration for hydrologic models: Comparison with multilevel expert calibration. *J. Hydrol. Eng* 4(2), 135–143.
23. Hargreaves, G.H., Samani, Z.A., 1985. Reference crop evapotranspiration from temperature. *Applied Engineering in Agriculture* 1 (2), 96–99

24. IPCC. 2007. *Climate Change 2007: Synthesis Report. An Assessment of the Intergovernmental Panel on Climate Change*. Cambridge: Cambridge University Press.
25. IPCC. 2012. Summary for Policymakers. In *Managing the Risks of Extreme Events and Disasters to Advance Climate Change Adaptation. A special Report of Working Groups I and II of the Intergovernmental Panel on Climate Change*: 1-19. Cambridge: Cambridge University Press.
26. IPCC. 2014. *Climate change 2014. Synthesis Report. Longer Report*.
27. Kebede, A., B. Diekkrüger, and S. Moges. 2014. Comparative Study of a Physically Based Distributed Hydrological Model versus a Conceptual Hydrological Model for Assessment of Climate Change Response in the Upper Nile, Baro-Akobo basin: a Case Study of the Sore watershed, Ethiopia. *Intl.J. River Basin Management*, 12(4): 299–318.
28. Kissi, A. E. 2014. *Flood Vulnerability Assessment in Downstream Area of Mono Basin, South-Eastern Togo: Yoto District*. Master's thesis, Université de Lomé.
29. Klassou, S. D. 1996. *Evolution climato-hydrologique récente et conséquences sur l'environnement : l'exemple du bassin versant du fleuve Mono (Togo-Bénin)*. PhD dissertation, Université de Bordeaux III.
30. Lawin, A.E. 2007. *Analyse climatologique et statistique du régime pluviométrique de la haute vallée de l'Ouémé à partir des données pluviographiques AMMA-CATCH Bénin*. Phd dissertation, Institut National Polytechnique de Grenoble ; Université d'Abomey-Calavi.
31. Lenderink, G., A. Buishand, and W. Van Deursen. Estimates of future discharges of the river Rhine using two scenario methodologies: direct versus delta approach. 2007. *Hydrology and Earth System Sciences*. 11(2007): 1145-1159.
32. Lundin, L-C., S. Bergström, E. Eriksson and J. Seibert. 2000. Hydrological Models and Modelling. In *Sustainable Water Management Book 1: The Waterscape*. Ed. Lars-Christer Lundin, 129-140. Uppsala University, Sweden.
33. Ly, S., C. Charles, and A. Degré. 2011. Geostatistical interpolation of daily rainfall at catchment scale: the use of several variogram models in the Ourthe and Ambleve catchments, Belgium. *Hydrology and Earth System Sciences*. 15(2011): 2259–2274.
34. Matheron, G. 1963. Principles of geostatistics. *Economic Geology* 58: 1246-1266
35. Mbaye, M.L., S. Hagemann, A. Haensler, T. Stacke, A.T. Gaye, and A. Afouda. 2015. Assessment of Climate Change Impact on Water Resources in the Upper Senegal Basin (West Africa). *American Journal of Climate Change* 4: 77-93.
36. Mbaye, M.L. 2015. *Assessment of climate change impact on water resources in the Sénégal river basin at Bakel*. Phd dissertation, Université d'Abomey-Calavi.

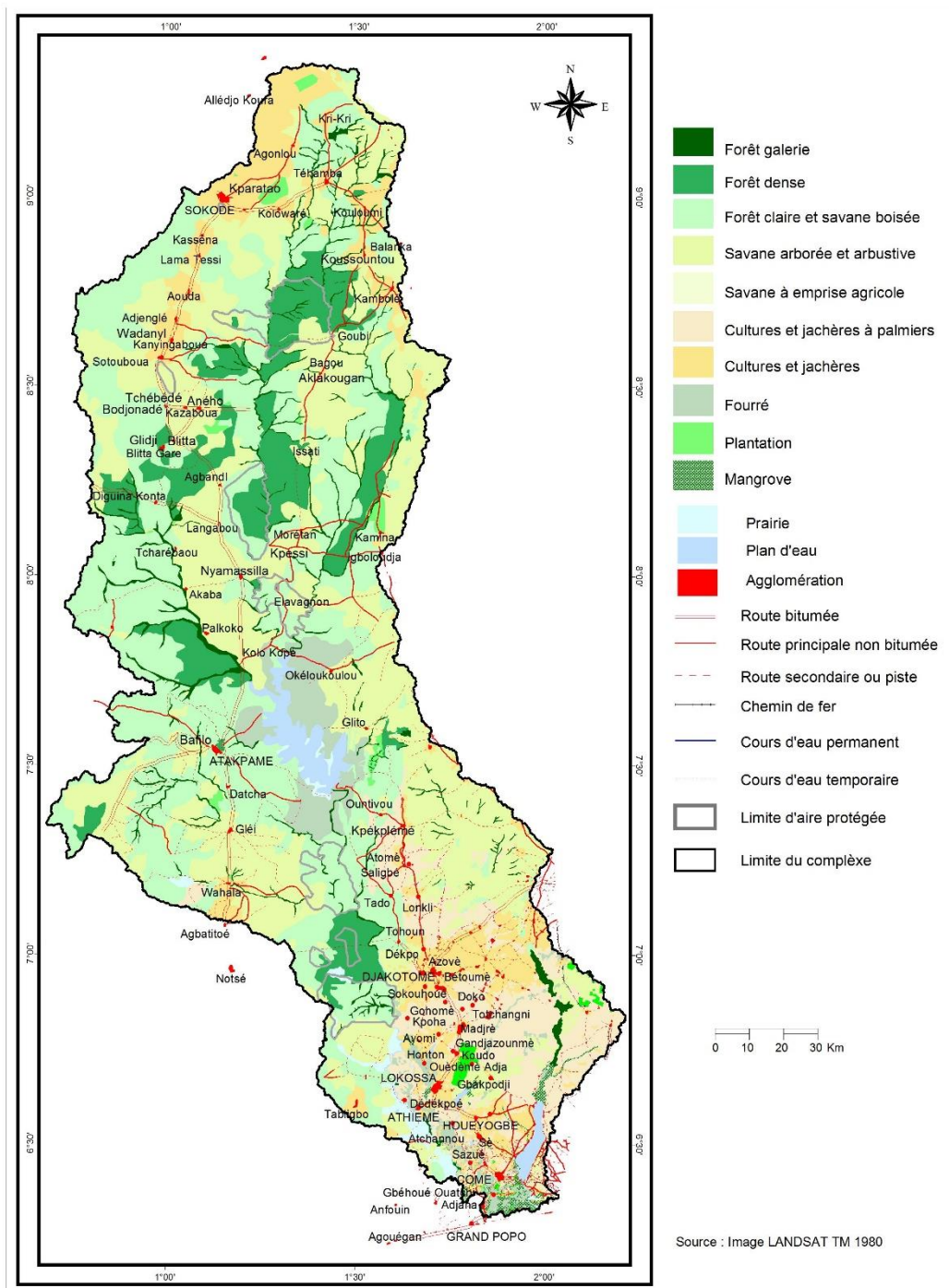
37. McKee, T.B., N.J. Doesken and J. Kleist. 1993. The relationship of drought frequency and duration to time scales. *Eighth Conference on Applied Climatology* 17-22 January 1993, Anaheim, California.
38. MEA. 2005. Ecosystems and Human Well-being: Wetlands and Water Synthesis. In *Millenium Ecosystem Assessment*. Washington, DC: World Research Institute.
39. Moss, R., M. Babiker, S. Brinkman, E. Calvo, T. Carter, J. Edmonds, I. Elgizouli, S. Emori, L. Erda, K. Hibbard, R. Jones, M. Kainuma, J. Kelleher, J. F. Lamarque, M. Manning, B. Matthews, J. Meehl, L. Meyer, J. Mitchell, N. Nakicenovic, B. O'Neill, R. Pichs, K. Riahi, S. Rose, P. Runci, R. Stouffer, D. van Vuuren, J. Weyant, T. Wilbanks, J. P. van Ypersele, and M. Zurek. 2008. *Towards New Scenarios for Analysis of Emissions, Climate Change, Impacts, and Response Strategies*. Intergovernmental Panel on Climate Change, Geneva.
40. Moss, R. H., J. A. Edmonds, K. A. Hibbard, M. R. Manning, S. K. Rose, D. P. van Vuuren, T. R. Carter, S. Emori, M. Kainuma, T. Kram, G. A. Meehl, J. F. B. Mitchell, N. Nakicenovic, K. Riahi, S. J. Smith, R. J. Stouffer, A. M. Thomson, J. P. Weyant, and T. J. Wilbanks. 2010. The next generation of scenarios for climate change research and assessment. *Nature* 463(11 February 2010).
41. Muhamad Ali, M.Z., and F. Othman. 2016. Selection of variogram model for spatial rainfall mapping using Analytical Hierarchy Procedure (AHP). *Scientia Iranica, Transactions A: Civil Engineering*. 24 (2017) 28-39.
42. Ntajal, J., B. L. Lamptey, and J. M. Sogbedji. 2016a. Flood Vulnerability Mapping in the Lower Mono River Basin in Togo, West Africa. *International Journal of Scientific and Engineering Research* 7(10): 1553-1562.
43. Ntajal, J., B. L. Lamptey, J. M. Sogbedji, and K. Wilson-Bahun. 2016b. Rainfall Trends and Flood Frequency Analyses in the Lower Mono River Basin in Togo, West Africa. *International Journal of Advance Research* 4(10).
44. N'Tcha M'Po, Y., A. E. Lawin, G. T. Oyerinde, B. K. Yao, and A. A. Afouda. 2016. Comparison of daily precipitation bias correction methods based on four regional climate model outputs in Ouémé Basin, Benin. *Hydrology*. 4(6): 58-71.
45. Obada, E., E.A. Alamou, A. Chabi, J. Zandagba, and A. Afouda. 2017. Trends and changes in recent and future Penman-Monteith potential evapotranspiration in Benin (West Africa). *Hydrology*. 4(38): 2-18

46. Oudin, L. 2004. *Recherche d'un modèle d'évapotranspiration potentielle pertinent comme entrée d'un modèle pluie-débit global*. Phd dissertation, Ecole Nationale du Génie Rural, des Eaux et des Forêts (ENGREF)
47. Oyerinde, G. T. 2016. *Climate change in the Niger basin on hydrological properties and functions of Kainji lake, West-Africa*. PhD dissertation, Université d'Abomey-Calavi.
48. Paturel, J. E., E. Servat, A. Dezetter, and J.F. Boyer. 2006. Modélisation Hydrologique et Régionalisation en Afrique de l'Ouest et Centrale. *IAHS* 307: 278–287.
49. Planton, S., P. Braconnot, C. Cassou, JL Dufresne, S. Hallegatte, and D. Salas Y Melia. 2013. Les Nouveaux Scénarios Climatiques du GIEC. *Pollution Atmosphérique*, numero special juin 2013: 32-39.
50. Rossi, G. 1989. L'érosion du littoral dans le Golfe du Bénin : Un exemple de perturbation d'un équilibre morphodynamique. *Z. Géomorph. N. F. Suppl.* Bd 73, pp 139-165.
51. Rossi, G., and A. Blivi. 1995. Les conséquences des aménagements hydrauliques de la vallée du Mono (Togo-Bénin). S'aura-t-on gérer l'avenir ? *Cahier d'Outre-Mer*, 48(192), 435-452
52. Roudier P., A. Ducharne, and L. Feyen. 2014. Climate change impacts on runoff in West Africa: a review. *Hydrology and earth system sciences*, 18(2014): 2789–2801.
53. Sutcliffe, J. V., and B. S. Piper. 1986. Bilan Hydrologique en Guinée et Togo-Bénin. *Hydrol. Continent.*, 1 (1): 51–61.
54. Terink, W., R. T. W. L. Hurkmans, P. J. J. F. Torfs, and R. Uijlenhoet. Bias correction of temperature and precipitation data for regional climate model application to the Rhine basin. 2009. *Hydrology and earth system sciences discussion*. 6: 5377–5413,
55. Teutschbein, C. and J. Seibert. 2012 Bias correction of regional climate model simulations for hydrological climate-change impact studies: Review and evaluation of different methods, *Journal of Hydrology*, 456–457 (2012) 12–29
56. Trambly, Y., E. Amoussou, W. Dorigi, G. Mahé. 2014. Flood Risk under Future Climate in Data Sparse Regions: Linking Extreme Value Models and Flood Generating Processes. *Journal of Hydrology* 519(2014): 549-558.
57. Trzaska; S., and E. Schnarr, 2014. *A review of downscaling methods for climate change projections: African and Latin American resilience to climate change (ARCC)*.
58. UNDP. 2011. *Inondations au Bénin: Rapport d'Evaluation des Besoins Post Catastrophe*. Cotonou, Benin.
59. United Nations. 1992. *United Nations Framework Convention on Climate Change (UNFCCC)*. New York.

60. United States Geological Survey (USGS). <https://water.usgs.gov/edu/dictionary.html>. Accessed on 07/06/2017.
61. van de Beek, C. Z., H. Leijnse, P. J. J. F. Torfs, and R. Uijlenhoet. 2011. Climatology of daily rainfall semi-variance in The Netherlands. *Hydrology and earth system sciences*. 15(2011): 171–183.
62. Varis, O., T. Kajander, and R. Lemmelä. 2004. Climate and water: from climate models to water resources management and vice versa. *Clim. Change* 66 (3), 321–344.
63. Verworn, A. and U. Haberlandt. 2011. Spatial interpolation of hourly rainfall effect of additional information, variogram inference and storm properties, *Hydrology and earth system sciences*. 15(2011): 569–584.
64. Wetterhall, F. 2012. Conditioning model output statistics of regional climate model precipitation on circulation patterns. *Nonlin. Processes Geophys.* 2012. (19):623–633.
65. World Meteorological Organization (WMO). <http://www.wmo.int/pages/prog/wcp/ccl/faqs.php>. Accessed on 07/06/2017
66. World Meteorological Organization (WMO). 2012. *Standardized precipitation index user guide*. Geneva, Switzerland.
67. Xu, C-y. 2002. *Textbook of Hydrologic Models*. Uppsala University, Sweden.
68. Xu, H. and Y. Luo. (2015). Climate change and its impacts on river discharge in two climate regions in China. *Hydrology and earth system sciences*. 19(2015): 4609–4618.
69. Xu, Y. 2017. Package Hyfo. *R repository RCRAN*. <https://yuanchao-xu.github.io/hyfo/>

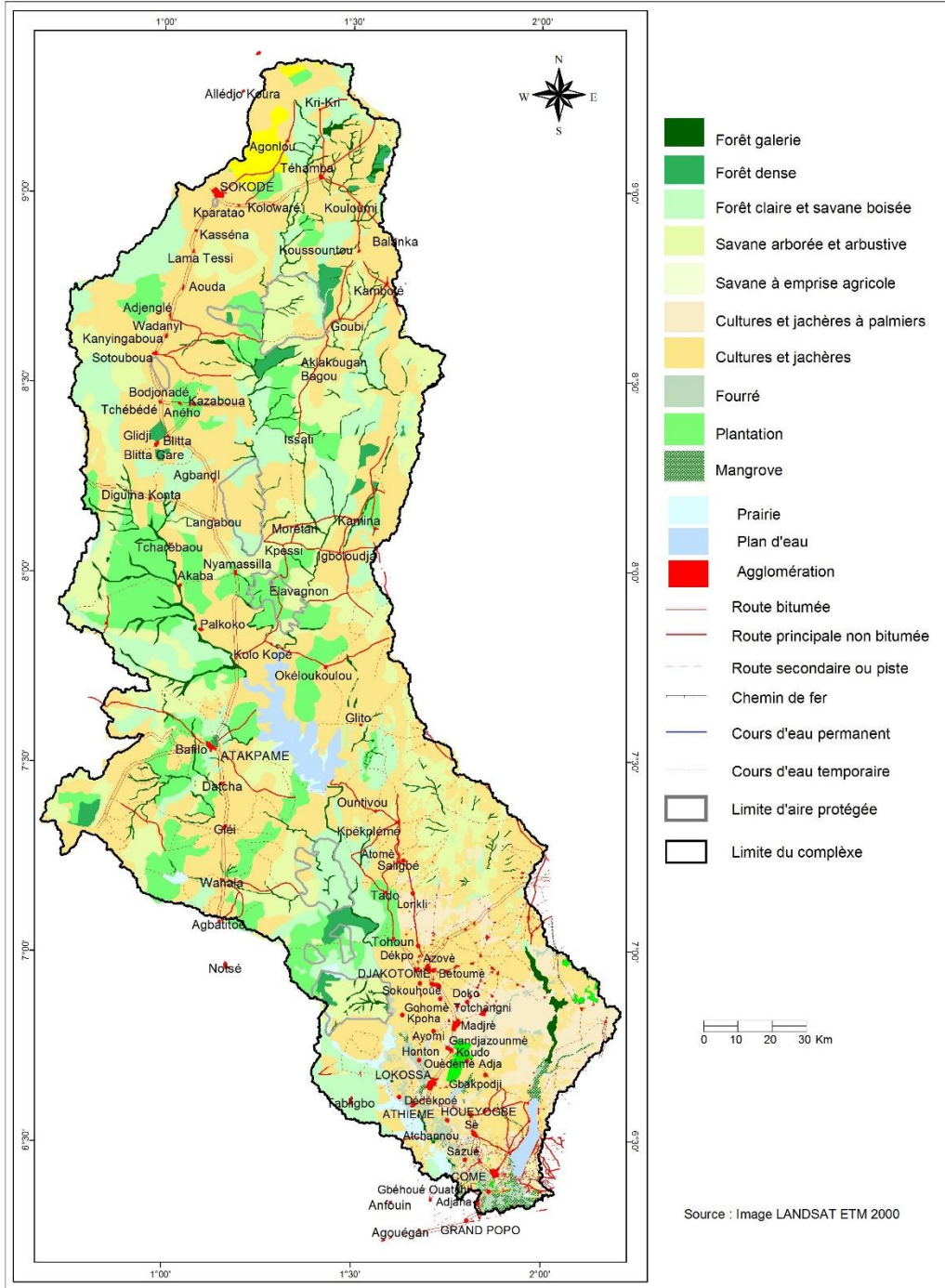
Annexes

Annex 1: Land use / land cover in Mono watershed for year 1980



Source : Benin Remote Sensing Centre, CENATEL (Centre National de Télédétection et de Suivi Ecologique)

Annex 2: Land use / land cover in Mono watershed for year 2015



Source : Benin Remote Sensing Centre, CENATEL (Centre National de Télédétection et de Suivi Ecologique)